# Magnetic quantum oscillations of in-plane Hall conductivity and magnetoresistance tensor in quasi-two-dimensional metals

P.D. Grigoriev<sup>1,2,3</sup> and T.I. Mogilyuk<sup>4</sup>

<sup>1</sup>L. D. Landau Institute for Theoretical Physics, Chernogolovka, 142432, Russia
 <sup>2</sup>National University of Science and Technology «MISiS», Moscow, 119049, Russia
 <sup>3</sup>Kotelnikov Institute of Radioengineering and Electronics of RAS, 125009 Moscow, Russia
 <sup>4</sup>National Research Centre «Kurchatov Institute», Moscow, 123182, Russia
 (Dated: June 10, 2024)

We develop the theory of magnetoresistance oscillations in layered quasi-two-dimensional (quasi-2D) metals. Using the Kubo-Streda formula, we calculate the Hall intralayer conductivity in a magnetic field perpendicular to conducting layers. The analytical expressions for the amplitudes and phases of magnetic quantum oscillations (MQO) and of the difference or the so-called slow oscillations (SO) are derived as a function of several parameters: magnetic field strength, interlayer transfer integral, temperature, the Landau-level broadening and the electron mean-free time. We calculate the quantum oscillations of the magnetoresistance tensor, because the magnetoresistance rather than conductivity is usually measured. We also discuss the averaging of magnetoresistance oscillations over temperature and long-range sample inhomogeneities. The results obtained are useful to analyze experimental data on magnetoresistance oscillations in various quasi-2D metals.

#### I. INTRODUCTION

Layered quasi-two-dimensional (quasi-2D) metals form a vast class of materials, promising both for research and applications. This class includes high- $T_c$  superconductors, both of cuprate and iron-based families, organic metals, various van-der-Waals crystals, intercalated graphite, artificial heterostructures, transition metal and rare-earth chalcogenides, etc. A huge amount of current research is devoted to the study of electronic structure in these materials. There are two main methods to measure the electronic structure in the bulk of these materials: angle-resolved photoemission spectroscopy (ARPES) [1] and magnetic quantum oscillations (MQO) [2-4]. ARPES is more visual than MQO, but has a poorer energy and momentum resolution and requires a high quality sample surface and sophisticated technique. The APRES resolution is often insufficient to study fine energy splitting and Fermi-surface (FS) reconstruction by electronic phase transitions. The MQO provide a tool to measure the FS geometry with much higher accuracy than ARPES and also give information about the effective mass, mean free time and g-factor of charge carries [2–4]. However, the extraction of this information from the experimental data on MQO requires a quantitative theory of MQO. The characteristic feature of MQO is their high sensitivity to temperature and disorder, including macroscopic sample inhomogeneities.

The electron spectrum in layered quasi-2D metals is usually described by a three-dimensional tight-binding dispersion

$$\epsilon_{3D}(\mathbf{k}) = \epsilon_{\parallel} (\mathbf{k}_{\parallel}) - 2t_z \cos(k_z d),$$
 (1)

where  $t_z$  is the interlayer transfer integral of electrons and d is the interlayer distance. The in-plane electron dispersion  $\epsilon_{\parallel}(\mathbf{k}_{\parallel})$  is often isotropic and can be approximated

by a parabolic one:

$$\epsilon_{\parallel} \left( \mathbf{k}_{\parallel} \right) = \hbar^2 \left( k_x^2 + k_y^2 \right) / (2m_*), \tag{2}$$

where  $m_*$  is the effective (cyclotron) electron mass. The FS of layered metals related to Eq. (1) is a corrugated cylinder. This Fermi surface has two close extremal crosssections areas  $S_1$  and  $S_2$  by the planes in k space perpendicular to the magnetic field B. The standard Lifshitz-Kosevich (L-K) theory in quasi-2D metals predicts that for each FS pocket the MQO are determined by the sum of oscillations with two close fundamental frequencies  $F_{1,2} = cS_{1,2}/(2\pi|e|\hbar)$  and almost equal amplitudes [2-4]. This leads to the amplitude beats of MQO with average frequency  $F = (F_1 + F_2)/2$ . The beat frequency  $\Delta F \equiv F_1 - F_2 \approx 4t_z B_z/(\hbar \omega_c)$  can be used to measure the interlayer transfer integral  $t_z$  [2, 5–8]. The phases of MQO beats in transport (across the layers) and thermodynamic quantities differ [9]. This phase shift increases with magnetic field [9–11] and reaches almost  $\pi/2$  in some quasi-2D metals [11, 12].

The particular angular dependence of the beat frequency  $\Delta F$ , i.e. its dependence on the tilt angle  $\theta$  of magnetic field from the normal to conducting (x, y) layers, allows to evaluate the in-plane Fermi momentum  $k_F$  [5–10]:

$$\Delta F(\theta)/\Delta F(0) = t_z(\theta)/t_z(0) = J_0(k_F d \tan(\theta)). \tag{3}$$

The beat frequency vanishes in the so-called Yamaji angles  $\theta_{\rm Yam}$  found from the zeros of the Bessel function in Eq. (3). The angular oscillations of the effective interlayer transfer integral  $t_z(\theta)$  described by Eq. (3) also lead to angular oscillations of magnetoresistance (AMRO). AMRO were first discovered in a quasi-2D organic metal  $\beta$ -(BEDT-TTF)<sub>2</sub>IBr<sub>2</sub> in 1988 [13] and explained by Yamaji using geometrical arguments [14]. This effect was quantitatively described next year using the Boltzmann transport equation [15]. Subsequently,

AMRO were widely analyzed in both quasi-2D and quasione-dimensional organic metals [5–9, 15–19] to extract useful information about the electronic dispersion, as well as in many other layered materials, including high-Tc superconductors [20] and artificial heterostructures [21]. The interplay of angular and quantum magnetoresistance oscillations is not trivial and leads to new effects [19, 22]. These two effects do not simply factorize in strong magnetic fields [19], as one often assumes to describe experimental results. One of such new effects resulting from the interplay of MQO and AMRO are the so-called false spin zeros, that may lead to incorrect estimates of the electron g-factor from the angular dependence of MQO. This effect survives and becomes even stronger in the presence of additional electronic states on the Fermi surface [22, 23], e.g., as in multiband compounds. Note that the antiferromagnetic ground state also strongly affects the g-factor of conducting electron and often leads to its nullification as measured from the MQO [24].

In addition to magnetic quantum (Shubnikov) oscillations, in quasi-2D metals there are also differencefrequency or the so-called slow oscillations (SO) of magnetoresistance. The SO were first discovered in 1988 while studying the organic superconductor  $\beta$ -(BEDT- $TTF)_2IBr_2$  [13, 25]. Similar oscillations have also been observed in other organic conductors, e.g.,  $\beta$ - $(BEDT-TTF)_2I_3$ ,  $\kappa$ - $(BEDT-TTF)_2Cu_2(CN)_3$  [26], and  $\kappa$ -(BEDT-TSF)<sub>2</sub>C(CN)<sub>3</sub> [27, 28]. The SO were also discovered in rare-earth metal tritellurides [29, 30]. SO can also occur in a bilayer structure despite the absence of  $k_z$  dispersion, for example, in cuprate superconductors [30–32]. The first theoretical explanation with the help of the Boltzmann equation was given in the work [33]. SO arise due to the corrugation of the Fermi surface of quasi-2D metals. Their frequency  $F_{SO} = 2\Delta F$  is equal to the doubled beat frequency. It is also proportional to the tunnel integral  $t_z$  and has the same angular dependence given by Eq. (3), as has been shown both theoretically and experimentally [33]. It was also shown that magnetization and seemingly other thermodynamic properties of quasi-2D metals have no SO in the case of noninteracting electrons [10, 33, 34]. These types of oscillations are much more resistant to a temperature increase and to macroscopic sample inhomogeneities since the SO frequency does not depend on the Fermi energy. Hence, the observation of SO is often easier than of Shubnikov oscillations [10, 30, 32, 33].

From the analysis of SO, one can find the interlayer transfer integral  $t_z$ , giving the electron hopping rate between the conducting layers, the mean free time  $\tau_0$  of electrons, the type of disorder in the system, etc [10, 32, 33]. When the SO originate from the  $k_z$  electron dispersion the angular dependence of SO frequency allows the evaluation of the in-plane Fermi momentum  $k_F$ . The SO originating from the interlayer electron hopping resemble the magnetic intersubband oscillations in 2D metals [35, 36] or the difference-frequency oscillations [37] arising from several FS pockets. The main difference between the SO

and the magnetic intersubband or difference-frequency oscillations is that both frequencies  $F_{1,2} = S_{1,2}/(2\pi|e|\hbar)$ correspond to the same FS pocket. Hence, the SO appear even in single-band quasi-2D metals. In addition, the effective electron mass  $m_*$  and the cyclotron frequency  $\omega_c = |e|B/(m_*c)$  are the same for both frequencies  $F_{1,2}$ . Hence, the phase and frequency of SO are not sensitive to the Fermi level, and the SO are not damped by the smearing of Fermi level by temperature or long-range disorder. contrary to the difference-frequency oscillations given by Eq. (29) of Ref. [37]. The T-damping of SO occurs at considerably higher temperature and originates from the electron-phonon or electron-electron interaction, which affects the SO amplitude via the Dingle factor. The analytical expressions for the SO are also much simpler than for difference-frequency oscillations corresponding to different FS pockets.

The available theory of MQO in quasi-2D metals is built only for the diagonal magnetoconductivity, out-ofplane [9, 10, 33, 38] or in-plane [39], while the resistance is often measured experimentally. To analyze the measured in-plane magnetoresistance, one needs to know the Hall conductivity and invert the magnetoconductivity tensor. Here, we calculate the quantum oscillations of Hall conductivity and study the in-plane magnetoresistance tensor. The Hall component of magnetoresistance is also very important, as it is often measured in layered metals. For example, the first observation of quantum oscillations in high-Tc cuprate superconductors in 2007 [40] was on Hall coefficient. There are many other layered materials where the experimental data on Hall resistance oscillations require a quantitative theoretical analysis: a bulk Bi<sub>2</sub>Se<sub>3</sub> [41, 42], CaFeAsF [43], LaFeAsO<sub>0.9</sub>F<sub>0.1- $\delta$ </sub> [44], rare-earth tritellurides [45, 46], etc.

In this work we calculate the Hall conductivity and find the intralayer magnetoresistance tensor, which contains magnetic quantum oscillation. In Sec. II we describe our model and approximations. In Sec. III we calculate the Hall conductivity component, including the quantum and differential (slow) oscillations. In Sec. IV we calculate the resistivity tensor. In Sec. V we discuss the results, and give their summary in Sec. VI. Appendices provide the details of our calculations.

#### II. THE MODEL AND BASIC FORMULAS

We consider a layered quasi-2D metal with dispersion given by Eqs. (1), (2) placed in a magnetic field  $\mathbf{B}=(0,\,0,\,B)$  perpendicular to the conducting layers. The Landau-level (LL) quantization of in-plane motion leads to the new electron dispersion [2, 47]

$$\epsilon(n, k_z) = \hbar\omega_c(n + 1/2) - 2t_z \cos(k_z d), \tag{4}$$

where n is the LL index.

We use the Feynman diagram technique [48] and the self-consistent Born approximation (SCBA) to find the

electron self-energy function coming from the elastic scattering by short-range crystal defects. We neglect the interelectronic interaction and the influence of phonons. Then we apply the harmonic expansion of MQO and keep only the first- and second-order terms in the Dingle factor to obtain the analytical expressions for conductivity tensor

Previously, the MQO of diagonal interlayer  $\sigma_{zz}$  and intralayer diagonal conductivity  $\sigma_{xx}$  were calculated in the same approximations [10, 19, 39] in quasi-2D metals. These calculations have shown several notable differences between the MQO of  $\sigma_{zz}$  and of  $\sigma_{xx}$  [39]. First, the MQO of  $\sigma_{zz}$  gradually invert phase at  $t_z \sim \hbar \omega_c/(4\pi)$  while the  $\sigma_{xx}$  MQO do not. It means that in MQO of  $\sigma_{zz}$  and  $\sigma_{xx}$ have the opposite phase in the weak field and the same phase in the strong field. Second, in quasi-2D metals there is the phase shift of beats  $\sim \hbar \omega_c/t_z$  in the MQO of  $\sigma_{zz}$ , which may reach  $\pi/2$  [9, 11, 49, 50]. In  $\sigma_{xx}$  this phase shift of beats is negligible, being smaller by the parameter  $t_z/\mu \ll 1$ . Third, the amplitude of SO in  $\sigma_{xx}$ depends nonmonotonically on  $\omega_c \tau_0$  and even changes sign at  $\omega_c \tau_0 \approx \sqrt{3}$  [39]. Such a phase inversion and the vanishing of amplitude are absent in the SO of  $\sigma_{zz}$ . Hence, similar to MQO, the SO of intralayer  $\sigma_{xx}$  and interlayer  $\sigma_{zz}$  conductivity are in the same phase in strong field at  $\omega_c \tau_0 \gg 1$  and in opposite phase at  $\omega_c \tau_0 < 1$ . Does this sign change of SO amplitude also appear in Hall conductivity  $\sigma_{xy}$  and in the in-plane magnetoresistance  $\rho_{xx}$  and  $\rho_{xy}$ ? Does the in-plane magnetoresistance tensor have any new features? To answer these questions we need to calculate the in-plane magnetoresistance tensor in quasi-2D metals.

#### II.1. Kubo-Streda formula in quasi-2D metals

To find the Hall conductivity of a quasi-2D metals we examine the derivation of the Kubo-Streda formula [51] obtained for the conductivity tensor in 2D metals (for a detailed derivation see pp. 33-42 of Ref. [52])

$$\sigma_{xy} = -\sigma_{yx} = \int_{-\infty}^{+\infty} d\varepsilon \frac{dn_F(\varepsilon)}{d\varepsilon} \sigma_{xy}(\varepsilon) \equiv \sigma_{xy}^I + \sigma_{xy}^{II}, (5)$$

where  $n_F(\varepsilon) = (1 + \exp[(\varepsilon - \mu)/T])^{-1}$  is the Fermi distribution function,  $\varepsilon$  is the electron energy,  $\mu$  is the chemical potential, T is temperature,

$$\sigma_{\mu\nu}^{I}(\varepsilon) = \frac{-\hbar}{4\pi} Tr \left\langle \hat{\jmath}_{\mu} \left( G^{A} - G^{R} \right) \hat{\jmath}_{\nu} G^{R} - \hat{\jmath}_{\mu} G^{A} \hat{\jmath}_{\nu} \left( G^{A} - G^{R} \right) \right\rangle \text{and first harmonics [54]},$$
(6)

and

$$\sigma_{\mu\nu}^{II}(\varepsilon) = \frac{|e|}{4\pi i} Tr \left\langle \left( G^A - G^R \right) \left( \hat{r}_{\mu} \hat{\jmath}_{\nu} - \hat{\jmath}_{\mu} \hat{r}_{\nu} \right) \right\rangle, \tag{7}$$

where e = -|e| < 0 is electron charge,  $G^A$  and  $G^R$  are the advanced and retarded electron Green's functions,  $\hat{\jmath}_{\nu}$  is the operator of electron current in the direction  $\nu$ , and

 $\hat{r}$  is the coordinate operator. The trace in Eqs. (5)-(7) is over all states, including all bands and the reservoir states. The derivation of Eqs. (5)-(7) does not make any assumptions about the electron dispersion and is valid also for quasi-2D multiband metals.

One can simplify the last term  $\sigma_{\mu\nu}^{II}$  after integrating it by parts and taking into account the definition of electric current  $j_{\mu} = ev_{\mu} = e\partial\epsilon(\mathbf{p})/\partial p_{\mu}$ , the electron Hamiltonian with Peierls substitution of the vector potential in the symmetric gauge  $\mathbf{A} = (-y, x, 0) B/2$ , and the commutation relations  $[\hat{r}_x, \hat{v}_y] = [\hat{r}_y, \hat{v}_x] = 0$ . As a result one obtains the expression from the work [53] of P. Streda

$$\sigma_{xy}^{II} = ec \left. \frac{\partial N(\varepsilon)}{\partial B} \right|_{\varepsilon = \mu},$$
 (8)

where  $N(\varepsilon)$  is the total number of states below the energy  $\varepsilon$ , including all electron bands or reservoir states, and  $\mu$  is the chemical potential equal to the Fermi energy. Eq. (8) can also be used for quasi-2D metals as its derivation does not depend on the electron dispersion and on the number of energy bands (see Appendix A).

The next well-known formula [53]

$$\sigma_{xy}^{I} = -\omega_c \tau \sigma_{xx},\tag{9}$$

where the electron mean-free time  $\tau$  contains the MQO in contrast to  $\tau_0$ , is often used to calculate the Hall conductivity. The derivation of this formula (9), given in Appendix B, assumes a free electron model (parabolic dispersion) and the neglects the vertex corrections. The latter are negligible if the scattering is only by point-like impurities. As follows from the derivation in Appendix B, Eq. (9) holds for several conducting bands, and the scattering rate  $1/\tau = 2|\mathrm{Im}\Sigma|/\hbar$  in SCBA for point-like impurities contains the sum of the density of states from all bands and depends on the electron energy  $\varepsilon$  only.

#### II.2. Harmonic expansion

To proceed further, we assume strong harmonic damping of MQO and keep only zeroth and first MQO harmonics. In quasi-2D metals we also keep the SO term, which is of the second order in Dingle factor but may be stronger than the first harmonics at high temperature or in the presence of long-range inhomogeneity of Fermi energy. The weakly oscillating density of electronic states (DoS) in quasi-2D metals is given by the sum of zeroth and first harmonics [54],

$$\rho \approx \rho_0 \left[ 1 - 2R_D J_0(\lambda) \cos\left(\alpha\right) \right],\tag{10}$$

where the nonoscillating part of the 2D DoS (per one spin) per one band is  $\rho_0 = m_*/(2\pi\hbar^2 d)$ . Here the generalized Dingle factor  $R_D \equiv \exp\left[-\pi/(\omega_c\tau)\right] = \exp(-\gamma)$  has the MQO, because  $\gamma \equiv \pi/(\omega_c\tau)$  oscillates,  $\alpha = \alpha\left(\varepsilon\right) \equiv 2\pi\left[\varepsilon - \text{Re}\Sigma^R(\varepsilon)\right]/(\hbar\omega_c)$  also oscillates because the electron self-energy  $\Sigma^R(\varepsilon)$  has MQO,  $\lambda \equiv 4\pi t_z/(\hbar\omega_c)$ ,  $J_0(\lambda)$ 

and  $J_1(\lambda)$  are the Bessel functions of the zeroth and first order.

To find  $\tau$ , we calculate the imaginary part of electron self-energy function, which in SCBA is proportional to the oscillating density of states:

$$\hbar/(2\tau) = \left| \operatorname{Im} \Sigma^{R}(\varepsilon) \right| = -\operatorname{Im} \Sigma^{R}(\varepsilon) \equiv \Gamma(\varepsilon)$$
 (11)

$$\approx \Gamma_0 \left[ 1 - 2R_D \cos \left[ \alpha(\varepsilon) \right] J_0(\lambda) \right]. \tag{12}$$

After neglecting the second harmonics but keeping the slow-oscillating term, this gives

$$\tau \equiv \frac{\hbar}{2\Gamma} \approx \tau_0 \left[ 1 + 2R_D J_0(\lambda) \cos(\alpha) + 2R_D^2 J_0^2(\lambda) \right]. \tag{13}$$

It was previously shown [10, 33, 39] that the combination  $R_D \cos(\alpha)$  does not contain the slow oscillations in the second order of Dingle factor. Therefore, as we are not interested in the second harmonic of MQO, all second-order terms coming from  $R_D \cos(\alpha)$  can be neglected both in the DoS and in  $\tau$ , and we have

$$\rho \approx \rho_0 \left[ 1 - 2R_{D0} J_0(\lambda) \cos\left(\overline{\alpha}\right) \right] = \rho_0 \left[ 1 + \widetilde{\rho}/\rho_0 \right], \quad (14)$$

$$\tau \approx \tau_0 \left[ 1 + 2R_{D0} \cos\left(\overline{\alpha}\right) J_0(\lambda) + 2R_{D0}^2 J_0^2(\lambda) \right]$$

$$\approx \tau_0 \left[ 1 - \widetilde{\rho}/\rho_0 + \tau_{SO}/\tau_0 \right], \quad (15)$$

where the Dingle factor  $R_{D0} \equiv \exp\left[-\pi/(\omega_c \tau_0)\right]$  does not oscillate,  $\overline{\alpha} = 2\pi\varepsilon/(\hbar\omega_c)$ ,  $\tau_{SO} = 2R_{D0}^2J_0^2(\lambda)\tau_0$ , and we introduced the notation  $\widetilde{\rho}$  for the oscillating part of DoS, keeping only its first harmonic:

$$\widetilde{\rho}/\rho_0 \approx -2R_{D0}J_0(\lambda)\cos\left(\overline{\alpha}\right).$$
 (16)

### III. CALCULATIONS OF HALL CONDUCTIVITY

Experimentally one often divides the Hall conductivity  $\sigma_{xy}$  into three terms, corresponding to the monotonic part, usual MQO and the slow or differential oscillations:

$$\sigma_{xy}(\varepsilon) \approx \overline{\sigma}_{xy}(\varepsilon) + \sigma_{xy}^{QO}(\varepsilon) + \sigma_{xy}^{SO}(\varepsilon).$$
 (17)

Below we use Eqs. (5), (8), (9) and (15) to calculate each term in Eq. (17).

#### III.1. Calculation of $\sigma_{xy}^{I}$

We start from Eq. (9) and the necessary expressions for  $\sigma_{xx}$  at temperature T=0 we take from Eqs. (35), (39) and (45) of Ref. [39], rewriting them using the relation  $\gamma_0 = \pi/(\omega_c \tau_0)$ :

$$\sigma_{xx}(\varepsilon) \approx \overline{\sigma}_{xx}(\varepsilon) + \sigma_{xx}^{QO}(\varepsilon) + \sigma_{xx}^{SO}(\varepsilon).$$
 (18)

Here the nonoscillating term per one spin component is

$$\overline{\sigma}_{xx}(\varepsilon) \approx \frac{e^2}{4\pi\hbar d} \frac{\overline{\alpha}\gamma_0}{\gamma_0^2 + \pi^2} = \frac{\sigma_0}{1 + (\omega_c \tau_0)^2},$$
 (19)

where the Drude conductivity without magnetic field is

$$\sigma_0 = \frac{e^2 \overline{\alpha} \omega_c \tau_0}{4\pi^2 \hbar d} = \frac{e^2 \mu \tau_0}{2\pi \hbar^2 d} = \frac{e^2 \tau_0 n_e}{m_*}, \tag{20}$$

and the electron density  $n_e = \mu \rho_0$ . The quantum oscillations term in the first order in  $R_{D0}J_0(\lambda)$  is

$$\frac{\sigma_{xx}^{QO}(\varepsilon)}{\overline{\sigma}_{xx}} \approx -2R_{D0} \left[ \frac{2\pi^2 J_0\left(\lambda\right)}{\gamma_0^2 + \pi^2} \cos\left(\overline{\alpha}\right) - \frac{\lambda J_1(\lambda)}{\overline{\alpha}} \sin(\overline{\alpha}) \right]$$
(21)

$$= -2R_{D0} \left[ \frac{2(\omega_c \tau_0)^2 J_0(\lambda)}{1 + (\omega_c \tau_0)^2} \cos(\overline{\alpha}) - \frac{\lambda}{\overline{\alpha}} J_1(\lambda) \sin(\overline{\alpha}) \right],$$
(22)

and the last term in Eq. (18), responsible for SO, in the second order in  $R_{D0}J_0(\lambda)$  is

$$\frac{\sigma_{xx}^{SO}(\varepsilon)}{\overline{\sigma}_{xx}} \approx 2\pi^2 R_{D0}^2 J_0^2(\lambda) \frac{\pi^2 - 3\gamma_0^2}{(\gamma_0^2 + \pi^2)^2}$$
 (23)

$$=2R_{D0}^{2}J_{0}^{2}(\lambda)\frac{(\omega_{c}\tau_{0})^{2}\left[(\omega_{c}\tau_{0})^{2}-3\right]}{\left[1+(\omega_{c}\tau_{0})^{2}\right]^{2}}.$$
 (24)

At nonzero temperature the Eq. (22) should be multiplied by temperature damping factor

$$R_T = 2\pi^2 k_B T / (\hbar \omega_c) / \sinh[2\pi^2 k_B T / (\hbar \omega_c)]. \tag{25}$$

To calculate  $\sigma_{xy}^I$  we substitute  $\tau$  from Eq. (15) into the Eq. (9). First, from the formula (19) we find the nonoscillating Hall conductivity, corresponding to the Drude model:

$$\overline{\sigma}_{xy}^{I} = -\omega_c \tau_0 \overline{\sigma}_{xx} = -\frac{e^2}{4\hbar d} \frac{\overline{\alpha}}{\gamma_0^2 + \pi^2} = \frac{-\omega_c \tau_0 \sigma_0}{1 + (\omega_c \tau_0)^2}. \quad (26)$$

As we show below,  $\overline{\sigma}_{xy}^{II} = 0$ , and the total nonoscillating part  $\overline{\sigma}_{xy} = \overline{\sigma}_{xy}^{I}$ . Substituting  $\tau$  from Eq. (13) and Eq. (21) into the Eq. (9) we obtain

$$\sigma_{xy}^{IQO} \approx -2\omega_c \tau_0 R_{D0} \cos(\overline{\alpha}) J_0(\lambda) \overline{\sigma}_{xx} - \omega_c \tau_0 \sigma_{xx}^{QO}$$

$$\approx 2\overline{\sigma}_{xy} R_{D0} \left[ \frac{\gamma_0^2 - \pi^2}{\gamma_0^2 + \pi^2} J_0(\lambda) \cos(\overline{\alpha}) + \frac{\lambda}{\overline{\alpha}} J_1(\lambda) \sin(\overline{\alpha}) \right]. \tag{27}$$

The slow oscillating terms come from Eqs. (9), (15), and (18):

$$\sigma_{xy}^{SO}(\varepsilon) \approx \omega_c \tau_0 \overline{\sigma_{xx}^{QO} \widetilde{\rho}/\rho_0} + \overline{\sigma}_{xy} \tau_{SO}/\tau_0 - \omega_c \tau_0 \sigma_{xx}^{SO}, \quad (28)$$

where the upper bar in the first term means averaging over the period of MQO. As we show below in Sec. III.2,  $\sigma_{xy}^{II}$  does not contribute to SO, because the DoS does not have slowly oscillating term. Hence,  $\sigma_{xy}^{SO}=\sigma_{xy}^{ISO}.$ 

Substituting Eqs. (16), (21), (15) and (23) into (28), we obtain

$$\sigma_{xy}^{SO}(\varepsilon) \approx 2\overline{\sigma}_{xy}R_{D0}^2J_0^2(\lambda)\frac{\gamma_0^2(\gamma_0^2 - 3\pi^2)}{(\gamma_0^2 + \pi^2)^2}$$
 (29)

$$=2\overline{\sigma}_{xy}R_{D0}^{2}J_{0}^{2}(\lambda)\frac{1-3(\omega_{c}\tau_{0})^{2}}{\left[1+(\omega_{c}\tau_{0})^{2}\right]^{2}}.$$
 (30)

Eqs. (29), (30) show that the amplitude of SO of the Hall conductivity vanishes at  $\gamma_0 = \sqrt{3}\pi$  or  $\omega_c \tau_0 = 1/\sqrt{3}$ .

### III.2. Calculation of $\sigma_{xy}^{II}$

The total electron density is (see Appendix C)

$$N(\mu) = \int_0^{\mu} \rho(B, \, \varepsilon) d\varepsilon \approx \rho_0 \left[ \mu + \frac{e\hbar B}{\pi m_* c} R_{D0} J_0(\lambda) \sin{(\overline{\alpha})} \right], \tag{31}$$

where we have substituted Eq. (14). It is not evident that the lowest integration limit in Eq. (31) is 0, because the lowest Landau level contributes the electron DoS  $\rho(B,\varepsilon)$  even at  $\varepsilon < 0$  if  $t_z > \hbar \omega_c/4$ . The result (31) is very sensitive to this integration limit. The equivalence of Eq. (31) to the initial formula for the DoS given by Eq. (C1) is shown in Appendix C. Eqs. (8) and (31) give

$$\sigma_{xy}^{II} = ec \frac{\partial N(\varepsilon)}{\partial B} \approx \rho_0 \frac{e^2 \hbar}{\pi m_*} \frac{\partial}{\partial B} \left[ BR_{D0} J_0(\lambda) \sin(\overline{\alpha}) \right]. \tag{32}$$

Note that  $\sigma_{xy}^{II}$  does not contain nonoscillating terms. The are also no SO in  $\sigma_{xy}^{II}$ , because there are no SO terms in the DoS, and they do not appear in  $N(\mu)$  in Eq. (31). Using the relations

$$\frac{\partial R_{D0}}{\partial B} = R_{D0} \frac{\gamma_0}{B},\tag{33}$$

$$\frac{\partial J_0(\lambda)}{\partial B} = -J_1(\lambda) \frac{\partial \lambda}{\partial B} = J_1(\lambda) \frac{\lambda}{B},\tag{34}$$

$$\frac{\partial \sin\left(\overline{\alpha}\right)}{\partial B} = -\cos(\overline{\alpha})\frac{\overline{\alpha}}{B},\tag{35}$$

we find from Eq. (32)

$$\sigma_{xy}^{II} \approx \rho_0 \frac{e^2 \hbar}{\pi m_*} R_{D0} \left[ -\overline{\alpha} J_0(\lambda) \cos(\overline{\alpha}) + \lambda J_1(\lambda) \sin(\overline{\alpha}) + J_0(\lambda) (\gamma_0 + 1) \cos(\overline{\alpha}) \right]. \tag{36}$$

Using Eq. (26) and  $\rho_0 = m_*/(2\pi\hbar^2 d)$  we rewrite Eq. (36) as

$$\sigma_{xy}^{II} \approx 2\overline{\sigma}_{xy}R_{D0}\frac{\gamma_0^2 + \pi^2}{\pi^2} \left[ J_0(\lambda)\cos(\overline{\alpha}) - \overline{\alpha}^{-1} \left[ \lambda J_1(\lambda)\sin(\overline{\alpha}) + J_0(\lambda)(\gamma_0 + 1)\cos(\overline{\alpha}) \right] \right].$$
(37)

#### III.3. Total MQO of Hall conductivity

Combining Eqs. (27) and (37) we obtain the MQO of Hall conductivity

$$\sigma_{xy}^{QO} = \sigma_{xy}^{IQO} + \sigma_{xy}^{II} = \widetilde{\sigma}_{xy}^{QO} + \Delta_{\lambda}\sigma_{xy}^{QO} + \Delta_{\gamma}\sigma_{xy}^{QO}. \quad (38)$$

At  $\overline{\alpha} \gg \lambda$ ,  $\gamma_0$ , 1, corresponding to  $\mu \gg t_z$ ,  $\hbar/\tau$ ,  $\hbar\omega_c$ , one may keep only the first main term in the square brackets of Eqs. (27) and (37), which gives the dominant  $\widetilde{\sigma}_{xy}^{QO}$  MQO term in the leading order in  $\overline{\alpha}$ :

$$\widetilde{\sigma}_{xy}^{QO} \approx 2\overline{\sigma}_{xy}R_{D0}J_0(\lambda)\cos(\overline{\alpha})\left[\frac{\gamma_0^2 - \pi^2}{\gamma_0^2 + \pi^2} + \frac{\gamma_0^2 + \pi^2}{\pi^2}\right] 
= 2\overline{\sigma}_{xy}R_{D0}J_0(\lambda)\cos(\overline{\alpha})\frac{\gamma_0^2}{\pi^2}\frac{\gamma_0^2 + 3\pi^2}{\gamma_0^2 + \pi^2} 
= -\frac{\overline{\sigma}_{xy}}{(\omega_c\tau_0)^2}\frac{1 + 3(\omega_c\tau_0)^2}{1 + (\omega_c\tau_0)^2}\frac{\widetilde{\rho}}{\rho_0}.$$
(40)

This formula coincides with Eq. (3.25) of Ref. [55], but the oscillating DoS now contains an extra factor  $J_0(\lambda)$ . The remaining two terms in Eq. (38) are smaller by the factors  $\sim t_z/\mu$  and  $\sim \hbar \omega_c/\mu$ :

$$\Delta_{\lambda} \sigma_{xy}^{QO} \approx 2\overline{\sigma}_{xy} R_{D0} \frac{\lambda}{\overline{\alpha}} J_{1}(\lambda) \sin(\overline{\alpha}) \left[ 1 - \frac{\gamma_{0}^{2} + \pi^{2}}{\pi^{2}} \right] 
= -2\overline{\sigma}_{xy} R_{D0} \frac{\lambda}{\overline{\alpha}} \frac{\gamma_{0}^{2}}{\pi^{2}} J_{1}(\lambda) \sin(\overline{\alpha}) 
= -4\overline{\sigma}_{xy} \frac{R_{D0}}{(\omega_{c}\tau)^{2}} \frac{t_{z}}{\mu} J_{1}(\lambda) \sin(\overline{\alpha})$$
(41)

and

$$\Delta_{\gamma} \sigma_{xy}^{QO} \approx -2\overline{\sigma}_{xy} R_{D0} J_0(\lambda) \frac{\gamma_0^2 + \pi^2}{\pi^2} \frac{\gamma_0 + 1}{\overline{\alpha}} \cos(\overline{\alpha})$$
$$\approx \overline{\sigma}_{xy} \frac{\widetilde{\rho}}{\rho_0} \frac{\gamma_0^2 + \pi^2}{\pi^2} \frac{\gamma_0 + 1}{\overline{\alpha}}.$$
 (42)

The term  $\Delta_{\lambda}\sigma_{xy}^{QO}$  leads to the phase shift of MQO and to a non-zero MQO amplitude in the beat nodes, similar to its effect in  $\tilde{\sigma}_{xx}^{QO}$  given by Eqs. (39)-(42) of Ref. [39]. It may be notable in various compounds where the  $k_z$  dispersion amplitude  $4t_z$  is comparable to the Fermi energy. The term  $\Delta_{\gamma}\sigma_{xy}^{QO}$  slightly changes the amplitude of MQO and is only important in semimetals.

At finite T after the averaging over a thermodynamic ensemble Eqs. (40)-(42) are multiplied by the temperature damping factor  $R_T$  given by Eq. (25). Eqs. (26), (30) and (38)-(42) for  $\sigma_{xy}$ , together with Eqs. (18)-(24) for  $\sigma_{xx} = \sigma_{yy}$ , complete our calculations of the magnetic oscillations of the conductivity tensor and allow to find the resistivity tensor.

In Figs. 1 and 2 we compare the calculated MQO and SO of the in-plane Hall and diagonal components of conductivity tensor, given by Eqs. (38)-(42), (30) for  $\sigma_{xy}$  and Eqs. (18)-(24) for  $\sigma_{xx}$ , with its interlayer component given by Eqs. (43)-(45) and with the MQO of DoS given

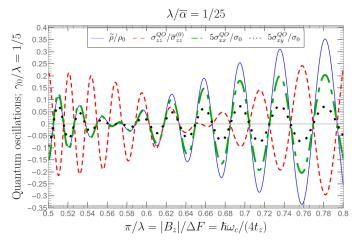


FIG. 1. Magnetic quantum oscillations at zero temperature of the density of states  $\widetilde{\rho}$ , interlayer conductivity  $\sigma_{xy}^{QO}$ , diagonal conductivity  $\sigma_{xx}^{QO}$  and Hall conductivity  $\sigma_{xy}^{QO}$  at  $\gamma_0/\lambda=1/5$  and  $\lambda/\overline{\alpha}=1/25$ . It can be seen that the oscillations of  $\widetilde{\rho}$ ,  $\sigma_{xx}^{QO}$ ,  $\sigma_{xy}^{QO}$  in the selected range of magnetic field are in phase and have the same beat-node positions. Meanwhile, the oscillations of  $\sigma_{zz}^{QO}$  and  $\widetilde{\rho}$  are mostly in antiphase except for the short interval  $|B_z|/\Delta F \in (0.57,\,0.66)$  between the beat nodes of  $\sigma_{xx}^{QO}$  and  $\sigma_{zz}^{QO}$ , because the latter is shifted.

by Eq. (16). The parameters for the plot in Fig. 1 are indicated in the figure and chosen to illustrate the behavior near the beat node. The MQO beat-node positions of  $\sigma_{xx}$ ,  $\sigma_{xy}$  and  $\tilde{\rho}/\rho_0$  coincide, while the beat-node position in  $\sigma_{zz}$  is shifted. The parameters for the plot in Fig. 2 are also indicated in the plot and chosen to illustrate the zero and sign change of the SO amplitude of  $\sigma_{xx}$  at  $\omega_c \tau_0 \approx \sqrt{3}$ , corresponding to  $|B_z|/\Delta F = \omega_c \tau_0 \gamma_0/\lambda \approx 0.35$  in Fig. 2.

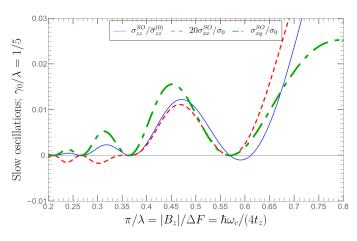


FIG. 2. Slow oscillations of interlayer conductivity  $\sigma_{zz}^{SO}$ , diagonal conductivity  $\sigma_{xx}^{SO}$  and Hall conductivity  $\sigma_{xy}^{SO}$  at  $\gamma_0/\lambda=1/5$ . The SO amplitude of diagonal in-plane conductivity  $\sigma_{xx}^{SO}$  changes its sign with phase inversion at  $|B_z|/\Delta F \approx 0.35$ . The SO of  $\sigma_{zz}$  are slightly shifted in phase according to Eq. (45).

#### IV. CALCULATION OF RESISTIVITY TENSOR

The resistivity tensor  $\hat{R} \equiv \hat{\sigma}^{-1}$  can be computed directly by the inversion of conductivity tensor  $\hat{\sigma}$  calculated in the previous section. However, a question appears about the correct order of two operations: the inversion of conductivity tensor and the temperature smearing. While this order does not affect the amplitude of the first MQO harmonic, it changes the higher harmonics and the differential slow oscillations. The correct order is not obvious and may depend on the physical system and even on the experimental setup. The same question about the temperature smearing of MQO appears for the longitudinal interlayer magnetoresistance  $R_{zz}(B_z) = \sigma_{zz}^{-1}(B_z)$ , as shown below.

### IV.1. Interlayer resistivity and its temperature averaging

The calculation of interlayer magnetoresistance  $R_{zz}(B_z)$  does not require inverting the in-plane conductivity tensor and is simpler than that of the in-plane magnetoresistance  $R_{xx}(B_z)$  or  $R_{xy}(B_z)$ . The interlayer magnetoconductivity in quasi-2D metals with SO is given by [10, 33, 39]

$$\sigma_{zz}(\mu, B_z) = \overline{\sigma}_{zz}^{(0)} + \sigma_{zz}^{QO}(\mu) + \sigma_{zz}^{SO}(\mu). \tag{43}$$

Here the monotonic part  $\overline{\sigma}_{zz}^{(0)}\left(B_{z}\right)$  depends on  $B_{z}$  only in a high magnetic field at  $\hbar\omega_{c} > \max\{4t_{z}, \pi\hbar/(2\tau_{0})\}$  when the SO are absent, and  $\hbar\omega_{c} \gg 4t_{z}, \hbar/\tau_{0}$  it has the asymptotic behavior  $\overline{\sigma}_{zz}^{(0)}\left(B_{z}\right) \propto B_{z}^{-1/2}$  according to Refs. [19, 56–59]. The MQO of  $\sigma_{zz} = \sigma_{zz}(\mu, B_{z})$  in the first order of the Dingle factor  $R_{D}$  are given by [10, 39]

$$\sigma_{zz}^{QO}(\mu, B_z) \approx 2\overline{\sigma}_{zz}^{(0)} \cos(\overline{\alpha}) R_{D0} R_T R_W \qquad (44)$$
$$\times \left[ J_0(\lambda) - \frac{2}{\lambda} (1 + \gamma_0) J_1(\lambda) \right],$$

where, by the analogy with Ref. [32], we add the factor  $R_W$  to describe the MQO damping by the phase smearing due to long-range spatial inhomogeneities [32, 33, 58]. The SO of  $\sigma_{zz}$  are given by Eq. (18) of Ref. [10] or Eq. (64) of Ref. [39]:

$$\sigma_{zz}^{SO}(\mu, B_z) \approx 2\overline{\sigma}_{zz}^{(0)} R_{D0}^2 J_0(\lambda) \left[ J_0(\lambda) - \frac{2}{\lambda} J_1(\lambda) \right]. \tag{45}$$

The interlayer resistivity in the lowest order in the Dingle factor is also given by the sum of three terms,

$$R_{zz} = \sigma_{zz}^{-1} = \overline{R}_{zz} + R_{zz}^{QO} + R_{zz}^{SO}, \tag{46}$$

where the monotonic term  $\overline{R}_{zz}=1/\overline{\sigma}_{zz}^{(0)}$  and the MQO of resistivity

$$R_{zz}^{QO}(\mu) \approx -2\overline{R}_{zz}\cos(\overline{\alpha}) R_{D0}R_T R_W$$

$$\times \left[ J_0(\lambda) - \frac{2}{\lambda} (1 + \gamma_0) J_1(\lambda) \right]$$
(47)

do not depend on the order of temperature smearing and of conductivity inversion. Only the second- and higher-order terms in  $R_D$ , including the term  $R_{zz}^{SO}$  describing the differential oscillations, depend on the order of these two operations.

If during the calculation of interlayer resistivity the temperature smearing is applied to the conductivity before its inversion (first method or  $\sigma$ -averaging), we obtain in the lowest second order in  $R_D$  the following SO term:

$$R_{zz}^{SO}/\overline{R}_{zz} \approx \left(\sigma_{zz}^{QO}/\overline{\sigma}_{zz}^{(0)}\right)^{2} - \sigma_{zz}^{SO}/\overline{\sigma}_{zz}^{(0)}$$

$$= -2R_{D0}^{2}J_{0}\left(\lambda\right)\left[J_{0}\left(\lambda\right) - \frac{2}{\lambda}J_{1}\left(\lambda\right)\right] +$$

$$+2R_{D0}^{2}\left(R_{T}R_{W}\right)^{2}\left[J_{0}\left(\lambda\right) - \frac{2}{\lambda}\left(1 + \gamma_{0}\right)J_{1}\left(\lambda\right)\right]^{2}.$$

$$(48)$$

If in the last line we assume  $(R_T R_W)^2 \ll 1$ , as it usually happens [33], we obtain

$$R_{zz}^{SO}/\overline{R}_{zz} \approx -2R_{D0}^2 J_0\left(\lambda\right) \left[J_0\left(\lambda\right) - \frac{2}{\lambda} J_1\left(\lambda\right)\right].$$
 (50)

It is this expression after the large-argument asymptotic expansion of the Bessel functions was used to analyze the experimental data in Ref. [33] and shown to be reasonably consistent.

If during the calculation of interlayer resistivity in Eq. (46) the smearing over temperature and sample inhomogeneities is applied to resistivity, i.e. only on the final step after the conductivity inversion (second method or R-averaging), we obtain

$$R_{zz}^{SO}/\overline{R}_{zz} \approx -2R_{D0}^{2}J_{0}\left(\lambda\right)\left[J_{0}\left(\lambda\right) - \frac{2}{\lambda}J_{1}\left(\lambda\right)\right] +$$

$$+2R_{D0}^{2}\left[J_{0}\left(\lambda\right) - \frac{2}{\lambda}\left(1 + \gamma_{0}\right)J_{1}\left(\lambda\right)\right]^{2}$$

$$\approx -\frac{8}{\lambda}R_{D0}^{2}J_{1}\left(\lambda\right)\left[\left(1/2 + \gamma_{0}\right)J_{0}\left(\lambda\right) - J_{1}\left(\lambda\right)\left(1 + \gamma_{0}\right)^{2}/\lambda\right].$$
(51)

The SO described by Eq. (51) are smaller than those in Eq. (50) by a factor  $\sim 2/\lambda$  and have a different phase. The usual Shubnikov oscillations  $R_{zz}^{QO}$ , given by Eq. (47), in the lowest main order in  $R_{D0}$  do not depend on the sequence of temperature averaging and conductivity inversion. Hence, by the comparison of the phase of SO and of the beats of Shubnikov oscillations one can experimentally determine what type of temperature averaging one should apply for the particular physical case. Unfortunately, in Ref. [33] no comparison of SO phase with the phase of MQO beats was performed.

Besides the temperature, the long-range (macroscopic) sample inhomogeneities result to the local variations of the Fermi energy  $\mu$  and of the MQO phase [32, 33, 58]. They give a major contribution to the MQO damping, described by the factor  $R_W$  in Eq. (44), and to the Dingle temperature in organic metals, as observed by the

comparison of the Dingle factors of usual MQO (fast oscillations) and differential SO (slow oscillations) [33]. Since the SO are not damped by such macroscopic inhomogeneities, they are often much stronger than the usual MQO [32, 33], because the Dingle temperature of SO is considerably smaller than that of MQO. The macroscopic Fermi-energy inhomogeneities also result to the Gaussian shape of Landau levels and to the strong modification of the field and harmonic dependence of the observed Dingle factor of MQO [58]. Averaging of resistivity or conductivity MQO over these inhomogeneities corresponds to their serial and parallel connection correspondingly. In real crystals these inhomogeneities appear in all directions, both parallel and perpendicular to the electric current. Hence, to describe these inhomogeneities it may be correct to average neither resistivity nor conductivity but an intermediate quantity, corresponding to an effective conductivity of a heterogeneous media [60].

A related question emerged in Ref. [58], where the measured field dependence of interlayer magnetoresistance  $R_{zz}$  ( $B_z$ ) in the quasi-2D organic metal  $\alpha$ -(BEDT-TTF)<sub>2</sub>KHg(SCN)<sub>4</sub> was compared to the theoretical prediction [56, 57] for its monotonic part  $\overline{R}_{zz}$  ( $B_z$ )  $\propto \sqrt{B_z}$ . In a high magnetic field the experimental curve  $R_{zz}$  ( $B_z$ ) contains strong MQO. Its averaging over the MQO period to extract the monotonic part  $\overline{R}_{zz}$  ( $B_z$ ) can be performed in two ways, depending on whether the resistance  $R_{zz}$  or conductivity  $\sigma_{zz} = R_{zz}^{-1}$  must be averaged. This example shows that in addition to the method of averaging of theoretical results, described by Eqs. (49)-(51), the averaging of experimental data over the MQO period is also important for their correct comparison with theory.

#### IV.2. In-plane resistivity tensor

As we have shown above, the question about the correct way of temperature averaging can be answered experimentally for any particular system. Below we give the result for both methods of temperature averaging. The resistivity tensor  $\hat{R} \equiv \hat{\sigma}^{-1}$  can be calculated directly using the results of previous section. Similar to Eq. (38), we separate the main oscillating term  $\hat{\sigma}_m$  and the small correction  $\Delta_{\lambda}\hat{\sigma}^{QO} \sim (2t_z/\mu)\,\hat{\sigma}$ .

The main terms in Eqs. (18)-(24) for  $\sigma_{xx} = \sigma_{yy}$  together with Eqs. (26), (30) and (38)-(40) for  $\sigma_{xy} = -\sigma_{xy}$  give the following in-plane conductivity tensor

$$\frac{\hat{\sigma}_m}{\overline{\sigma}_{xx}} = \begin{pmatrix} A_{xx} & A_{xy} \\ A_{yx} & A_{yy} \end{pmatrix}, \tag{52}$$

where the diagonal term is

$$A_{xx} \approx 1 + \frac{2(\omega_c \tau_0)^2}{1 + (\omega_c \tau_0)^2} \frac{\tilde{\rho}}{\rho_0} R_T R_W$$

$$+2R_{D0}^2 J_0^2(\lambda) \frac{(\omega_c \tau_0)^2 \left[ (\omega_c \tau_0)^2 - 3 \right]}{\left[ 1 + (\omega_c \tau_0)^2 \right]^2},$$
(53)

the off-diagonal term is

$$A_{xy} \approx -\omega_c \tau_0 \left( 1 - \frac{R_T R_W}{(\omega_c \tau_0)^2} \frac{1 + 3(\omega_c \tau_0)^2}{1 + (\omega_c \tau_0)^2} \frac{\tilde{\rho}}{\rho_0} + \frac{2R_{D0}^2 J_0^2(\lambda)(1 - 3(\omega_c \tau_0)^2)}{[1 + (\omega_c \tau_0)^2]^2} \right), \tag{54}$$

and the conductivity tensor has the following symmetry properties:

$$A_{xy} = -A_{yx}, \ A_{yy} = A_{xx}. (55)$$

The formal inversion of the conductivity tensor in Eq. (52) gives the following resistivity tensor

$$\hat{R} \equiv \hat{\sigma}^{-1} = \frac{1}{\sigma_0} \begin{pmatrix} B_{xx} & B_{xy} \\ B_{yx} & B_{yy} \end{pmatrix}, \text{ where}$$
 (56)

$$B_{xx} \approx 1 + 2\frac{\widetilde{\rho}}{\rho_0} R_T R_W + \frac{2R_{D0}^2 J_0^2(\lambda) \left[ (\omega_c \tau_0)^4 - R_T^2 R_W^2 \right]}{(\omega_c \tau_0)^2 \left[ 1 + (\omega_c \tau_0)^2 \right]},$$
(57)

$$B_{xy} \approx \omega_c \tau_0 - \frac{\widetilde{\rho} R_T R_W}{\omega_c \tau_0 \rho_0} +$$

$$\frac{2R_{D0}^{2}J_{0}^{2}(\lambda)\left[(\omega_{c}\tau_{0})^{2}-R_{T}^{2}R_{W}^{2}\left[3+4(\omega_{c}\tau_{0})^{2}\right]\right]}{\omega_{c}\tau_{0}\left[1+(\omega_{c}\tau_{0})^{2}\right]},\quad(58)$$

$$B_{xy} = -B_{yx}, B_{yy} = B_{xx}. (59)$$

Here we expanded the result in the powers of  $R_{D0}$ , and in the second order in  $R_D$  we only kept the SO terms. According to these formulas, the MQO of diagonal and Hall magnetoresistance components, given by the second terms in Eqs. (57) and (58), have opposite phase. This does not depend on the averaging procedure, because the MQO appear in the first order of the Dingle factor. The resistivity MQO given by Eqs. (47) and (73)-(76) are shown in Figs. 3 and 6. The SO of diagonal and Hall magnetoresistance components may have the same or opposite phase, depending on the averaging procedure, on magnetic field strength, and on damping factors  $R_T R_W$ .

#### IV.2.1. Resistivity tensor for $\sigma$ -averaging

For  $\sigma$ -averaging the resistivity tensor is given by Eqs. (56)-(59), where the damping factors  $R_T$  and  $R_W$  in the SO terms of Eqs. (57) and (58) are the same as in the second MQO terms. Hence, for this type of averaging the mutual phase and the amplitudes of  $R_{xx}$  and  $R_{xy}$  SO can be controlled by temperature and magnetic field strength. Unlike  $\sigma_{xx}$  and  $\sigma_{xy}$  SO oscillations, given by Eqs. (24) and (30), the zero point where the amplitude of resistivity SO in Eqs. (57) and (58) vanishes, for  $\sigma$ -averaging depends on temperature and on spatial heterogeneity via the suppression factor  $R_T R_W$ .

According to Eq. (57), the amplitude of the SO of diagonal components  $R_{xx} = R_{yy}$  vanishes at

$$\omega_c \tau_0 = \sqrt{R_T R_W}. \tag{60}$$

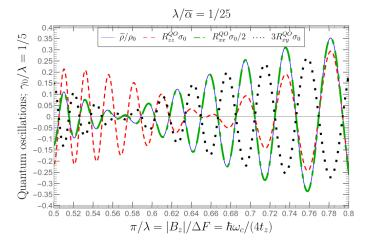


FIG. 3. Magnetic quantum oscillations at zero temperature of the density of states  $\widetilde{\rho}$ , interlayer resistivity  $R_{zz}^{QO}$ , diagonal resistivity  $R_{xx}^{QO}$  and Hall resistivity  $R_{xy}^{QO}$  at  $\gamma_0/\lambda=1/5$  and  $\lambda/\overline{\alpha}=1/25$ . The oscillations of  $\widetilde{\rho}$  and  $R_{xx}^{QO}$  are always in phase, while the  $R_{xy}^{QO}$  oscillations are antiphase with them. The oscillations of  $R_{zz}^{QO}$  are mostly in phase with  $\widetilde{\rho}$  and  $R_{xx}^{QO}$  except for the short interval  $|B_z|/\Delta F \in (0.56,\,0.67)$  near the beat node which is shifted for  $R_{zz}^{QO}$ .

This condition is rarely satisfied at any magnetic field  $B_z$ , because the product  $R_T R_W$  increases from an exponentially small value at  $\omega_c \tau_0 \ll 1$  to unity at  $\omega_c \tau_0 \gg 1$ , and usually  $R_T R_W \lesssim R_{D0} = \exp\left(-\pi/(\omega_c \tau_0)\right) \ll (\omega_c \tau_0)^2$  at all  $B_z$ . Only if  $R_T R_W > 20 R_{D0}$  at  $\omega_c \tau_0 \sim 1$  Eq. (60) can be satisfied, but, usually,  $R_T R_W < R_{D0}$ .

The amplitude of slow oscillations of non-diagonal components  $\rho_{xy}^R = -\rho_{yx}^R$  vanishes at some field  $B_z$  corresponding to

$$\omega_c \tau_0 = R_T R_W \sqrt{3/(1 - 4R_T^2 R_W^2)}. (61)$$

Formally, Eq. (61) always has a real solution, because  $R_T R_W$  depends on magnetic field  $B_z$ , and with the increase of  $B_z$  the right hand side of this equation increase from an exponentially small value at  $\omega_c \tau_0 \ll 1$  to infinity at  $\omega_c \tau_0 > 1$  when  $R_T R_W = 1/2$ . Nevertheless, if  $R_W \ll 1$  at the available magnetic field, the zero point of the SO amplitude of  $R_{xy}$  may happen at too high magnetic field, above the experimental window.

At  $R_T R_W \ll 1$  Eqs. (57) and (58) simplify to

$$B_{xx} \approx 1 + 2\frac{\tilde{\rho}}{\rho_0} R_T R_W + \frac{2R_{D0}^2 J_0^2(\lambda)(\omega_c \tau_0)^2}{1 + (\omega_c \tau_0)^2},$$
 (62)

$$B_{xy} \approx \omega_c \tau_0 - \frac{\widetilde{\rho} R_T R_W}{\omega_c \tau_0 \rho_0} + \frac{2\omega_c \tau_0 R_{D0}^2 J_0^2(\lambda)}{1 + (\omega_c \tau_0)^2}.$$
 (63)

In this limiting case the MQO of diagonal and Hall magnetoresistance components have opposite phase, and their SO have the same phase. Comparing Eqs. (62) and (63) with Eq. (50) we note that at  $R_T R_W \ll 1$  and  $2/\lambda = \hbar \omega_c/(2\pi t_z) \ll 1$  the phase of SO of  $R_{xx}$  and  $R_{xy}$  is nearly opposite to the SO phase of  $R_{zz}$ . This case is illustrated in Fig. 4.

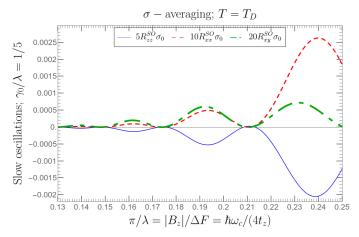


FIG. 4. Slow oscillations of interlayer resistivity  $R_{zz}^{SO}$ , diagonal resistivity  $R_{xx}^{SO}$  and Hall resistivity  $R_{xy}^{SO}$ , given by Eqs. (50) and (56)-(58) as a result of  $\sigma$ -averaging at temperature  $T=T_D$  and  $\gamma_0/\lambda=1/5$ . The slow oscillations  $R_{zz}^{SO}$  and  $R_{xx}^{SO}$  are in phase.

#### IV.2.2. Resistivity tensor at R-averaging

If the averaging over temperature and long-range spatial inhomogeneities is applied only to resistivity at the final stage, the  $R_T$  and  $R_W$  factors in the conductivity tensor given by Eqs. (52)-(54) should be replaced by unity before the tensor inversion. Hence, for R-averaging the resistivity tensor is again given by Eqs. (56)-(59), where the damping factors  $R_T$  and  $R_W$  appear only in the second MQO terms of Eqs. (57) and (58), while in the third SO terms of Eqs. (57) and (58) the factors  $R_T$  and  $R_W$  must be replaced by unity. The leading term of the in-plane resistivity tensor is then given by the matrix in Eq. (56) with the elements

$$B_{xx} \approx 1 + 2\frac{\widetilde{\rho}}{\rho_0} R_T R_W + 2R_{D0}^2 J_0^2(\lambda) \frac{(\omega_c \tau_0)^2 - 1}{(\omega_c \tau_0)^2},$$
 (64)

$$B_{xy} \approx \omega_c \tau_0 - \frac{R_T R_W}{\omega_c \tau_0} \frac{\widetilde{\rho}}{\rho_0} - \frac{6R_{D0}^2 J_0^2(\lambda)}{\omega_c \tau_0}.$$
 (65)

As can be seen from Eq. (64), for this averaging procedure the SO of the diagonal component  $R_{xx}$  of resistivity tensor vanish at  $\omega_c\tau_0=1$ , corresponding to  $\pi/\lambda\approx0.2$  in Fig. 5, while the amplitude of the SO of its Hall component  $R_{xy}$  does not have zeros. In a strong field at  $\omega_c\tau_0>1$  the SO of  $R_{xx}$  and  $R_{xy}$  have opposite phase, similar to MQO. In a weak field at  $\omega_c\tau_0<1$  the SO of  $R_{xx}$  and  $R_{xy}$  have the same phase, but in this limit the amplitude of SO  $\sim R_{D0}^2=\exp\left(-2\pi/(\omega_c\tau_0)\right)\ll1$  is small.

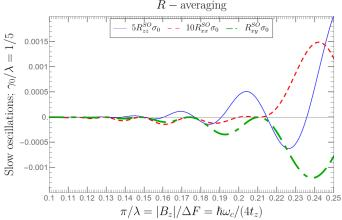


FIG. 5. Slow oscillations of interlayer resistivity  $R_{zz}^{SO}$ , diagonal resistivity  $R_{xx}^{SO}$  and Hall resistivity  $R_{xy}^{SO}$ , given by Eqs. (51), (64) and (65) as a result of R-averaging at  $\gamma_0/\lambda=1/5$ . Slow oscillations  $R_{zz}^{SO}$  and  $R_{xx}^{SO}$  are approximately shifted by a quarter of a period relative to each other. The SO oscillations  $R_{xx}^{SO}$  and  $R_{xy}^{SO}$  have the same phase in a weak magnetic field and opposite phases in a strong field, according to Eqs. (64) and (65).

# IV.3. Resistivity MQO with the corrections due to finite interlayer electron dispersion

Contrary to the slow oscillations, the MQO of resistivity tensor in the first order of Dingle factor do not depend on the averaging procedure and are given by the second terms in Eqs. (57) and (58), where  $\tilde{\rho}/\rho_0$  is given by Eq. (16). Combining Eqs. (56)-(58) and (16) we obtain the main MQO term of in-plane resistivity tensor

$$R_{xx}^{QO} \approx \frac{-4}{\sigma_0} R_{D0} R_T R_W J_0(\lambda) \cos(\overline{\alpha}),$$
 (66)

$$R_{xy}^{QO} \approx \frac{2R_{D0}R_TR_W}{\sigma_0\omega_c\tau_0}J_0(\lambda)\cos(\overline{\alpha}).$$
 (67)

These formulas take only the first main term in Eqs. (22), (27) and (37), neglecting the corrections  $\sim (\lambda/\overline{\alpha}) \sim 2t_z/\mu$  and  $\sim (\gamma+1)/\overline{\alpha}$ .

The small correction  $\Delta_{\lambda}\hat{\sigma}^{QO} \sim (\lambda/\overline{\alpha})\hat{\sigma} \sim 2t_z/\mu$  to conductivity tensor is obtained from Eqs. (22) and (41):

$$\frac{\Delta_{\lambda} \hat{\sigma}^{QO}}{\overline{\sigma}_{xx}} = \begin{pmatrix} \Lambda_{xx} & \Lambda_{xy} \\ \Lambda_{yx} & \Lambda_{yy} \end{pmatrix}, \text{ where}$$
 (68)

$$\Lambda_{xx} = \Lambda_{yy} \approx 2 \left( \lambda / \overline{\alpha} \right) R_{D0} R_T R_W J_1(\lambda) \sin(\overline{\alpha}), \quad (69)$$

$$\Lambda_{xy} = -\Lambda_{yx} \approx 2 \frac{R_{D0} R_T R_W}{\omega_c \tau_0} \frac{\lambda}{\overline{\alpha}} J_1(\lambda) \sin(\overline{\alpha}).$$
 (70)

We keep this correction for three reasons. First, it is not small when  $4t_z \sim \mu$ , i.e. when the  $k_z$  electron dispersion bandwidth is not much smaller than the Fermi energy. This case may be relevant to iron-based and cuprate high-Tc superconductors. The former have several small Fermi-surface (FS) pockets, warped due to the

 $k_z$  electron dispersion. The latter also have small FS pockets, as observed by MQO [40, 61, 62], coming from the FS reconstruction due to a charge-density wave [61] or antiferromagnetic ordering [62]. Second, the correction  $\sim \lambda/\overline{\alpha}$  gives a measurable phase shift of MQO, because in contains  $\sin(\overline{\alpha})$  instead of  $\cos(\overline{\alpha})$  in the main term. Third, it results to a nonzero MQO amplitude in the beat nodes. Below we omit the second small correction  $\Delta_{\gamma}\hat{\sigma}^{QO}\sim\hat{\sigma}\left(\gamma_{0}+1\right)/\overline{\alpha}$ , given by Eq. (42), as it is important only in semimetals with very few occupied LL, when  $\hbar\omega_{c}\sim\mu$ , and it does not lead to the phase shift of MQO.

The corrections to resistivity in the first order in  $\lambda/\overline{\alpha}=2t_z/\mu$  is also in the first order in Dingle factor  $R_{D0}$ . Hence, it does not depend on the temperature averaging procedure, similar to the usual MQO in the first order in  $R_{D0}$ . The inversion of conductivity tensor  $\hat{\sigma}+\Delta_\lambda\hat{\sigma}^{QO}$ , similar to that in the previous subsection, gives the correction to resistivity  $\Delta_\lambda\hat{R}$ , where the diagonal element

$$\Delta_{\lambda} R_{xx}^{QO} \approx \frac{2}{\sigma_0} \frac{\lambda}{\overline{\alpha}} R_{D0} R_T R_W J_1(\lambda) \sin(\overline{\alpha}), \quad (71)$$

and the off-diagonal element

$$\Delta_{\lambda} R_{xy}^{QO} \approx \frac{-2}{\sigma_0} \frac{\lambda}{\overline{\alpha}} \frac{R_{D0} R_T R_W}{\omega_c \tau_0} J_1(\lambda) \sin(\overline{\alpha}). \tag{72}$$

Combining Eqs. (66) and (67) with Eqs. (71) and (72) we obtain

$$R_{xx}^{QO} \approx \frac{-4R_{D0}R_TR_W}{\sigma_0} \sqrt{1 + \left(\frac{\lambda J_1(\lambda)}{2\overline{\alpha}J_0(\lambda)}\right)^2} J_0(\lambda) \cos\left(\overline{\alpha} + \phi_{xx}\right)_{\text{ity, given by Eqs. (73)-(76), are plotted in Fig. 6 in comparison with the MQO of DoS  $\widetilde{\rho}$  and of interlayer$$

where the phase shift  $\phi_{xx}$  is

$$\phi_{xx} = \arctan\left(\frac{\lambda J_1(\lambda)}{2\overline{\alpha}J_0(\lambda)}\right),$$
 (74)

and

$$R_{xy}^{QO} \approx 2 \frac{R_{D0} R_T R_W}{\omega_c \tau_0 \sigma_0} \sqrt{1 + \left(\frac{\lambda J_1(\lambda)}{\overline{\alpha} J_0(\lambda)}\right)^2} J_0(\lambda) \cos\left(\overline{\alpha} + \phi_{xy}\right), \tag{75}$$

where the phase shift  $\phi_{xy}$  is

$$\phi_{xy} = \arctan\left(\frac{\lambda J_1(\lambda)}{\overline{\alpha}J_0(\lambda)}\right).$$
 (76)

At  $\lambda/\overline{\alpha} = 2t_z/\mu \ll 1$  the phase shifts  $\phi_{xx} < \phi_{xy} \ll 1$  and Eqs. (73)-(76) give the same MQO as Eqs. (56)-(59).

Note that the MQO phase shift  $\phi_{xy}$  of Hall resistance is almost twice larger than the MQO phase shift  $\phi_{xx}$  of diagonal resistance components. This can be checked experimentally, if the diagonal  $R_{xx}$  and Hall  $R_{xy}$  magnetoresistance oscillations are measured simultaneously. The calculated correction  $\Delta_{\lambda} \hat{R}^{QO} \sim (2t_z/\mu) \hat{R}$  in resistivity is important even if it is small, because (i) it gives a

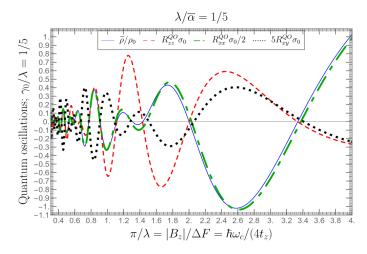


FIG. 6. Magnetic quantum oscillations of the density of states  $\widetilde{\rho}$  and of resistivity across  $R_{zz}^{QO}$  and along the conducting layers,  $R_{xx}^{QO}$  and  $R_{xy}^{QO}$ , given by Eqs. (16), (47) and (73)-(76) correspondingly, at  $\gamma_0/\lambda=1/5$  and  $\lambda/\overline{\alpha}=1/5$ . The MQO of  $\widetilde{\rho}$  and  $R_{xx}^{QO}$  are in phase, while the MQO of  $R_{xy}^{QO}$  are antiphase with them. The MQO of  $R_{zz}^{QO}$  have the same phase as  $\widetilde{\rho}$  and  $R_{xx}^{QO}$  in a weak magnetic field, but at  $B_z\sim\Delta F$  the MQO of  $R_{zz}^{QO}$  experience a 3D-2D crossover with a phase inversion according to Eq. (47) and Ref. [11]. The MQO amplitude of  $R_{xx}^{QO}$  and  $R_{xy}^{QO}$  at the beat nodes are not very small, being  $\sim \lambda/\overline{\alpha}=1/5$  of their amplitude far from the beat nodes.

measurable phase shift of resistivity MQO given by Eqs. (74) and (76), and (ii) it gives a nonzero MQO amplitude even in the beat nodes where  $J_0(\lambda) = 0$ .

The MQO of diagonal  $R_{xx}^{QO}$  and Hall  $R_{xy}^{QO}$  resistivity, given by Eqs. (73)-(76), are plotted in Fig. 6 in comparison with the MQO of DoS  $\tilde{\rho}$  and of interlayer resistivity  $R_{zz}^{QO}$ , given by Eqs. (16) and (47). The parameter  $\lambda/\bar{\alpha}=1/5$  in Fig. 6 is chosen rather large to illustrate the non-zero amplitude at the beat nodes. The MQO of  $\tilde{\rho}$  and  $R_{xx}^{QO}$  are in phase, while the MQO of  $R_{xy}^{QO}$  are antiphase with them. The MQO of  $R_{zz}^{QO}$  have the same phase as  $\tilde{\rho}$  and  $R_{xx}^{QO}$  in a weak magnetic field, but at  $B_z \sim \Delta F$  the MQO of  $R_{zz}^{QO}$  experience a 3D-2D crossover with a considerable phase shift of beats according to Eq. (47) and Ref. [11]. Therefore, the phase of  $R_{zz}^{QO}$  is opposite to the phase of  $\tilde{\rho}$  and  $R_{xx}^{QO}$  in wide  $B_z$  intervals, e.g. at  $B_z > 0.15\Delta F$  in Fig. 6. At  $B_z > \Delta F$  the MQO phase of  $R_{zz}^{QO}$  always coincides with that of DoS  $\tilde{\rho}$ , but we don't reach this interval in Fig. 6.

#### V. DISCUSSIONS

For the experimental study of the in-plane electronic transport in quasi-2D metals, especially in a magnetic field, usually, one applies the van-der-Pauw method [63, 64] or its extension – the Montgomery method [65]. Both these techniques measure the in-plane resistivity tensor rather than conductivity. Therefore, our calculations of the resistivity tensor performed in Sec. IV are

necessary to describe the experimental data on MQO and SO in quasi-2D metals. This requires the calculation of Hall conductivity in addition to its diagonal component calculated earlier [39], which is performed in Sec. III. There is a vast amount of experiments on in-plane magnetoresistance in layered quasi-2D metals, including various high-Tc superconductors [40, 66], rare-earth tritellurides [30, 67, 68], graphite flakes [69], and many other materials. Our analytical results are useful and convenient to analyze these experimental data.

To calculate the resistivity tensor, which we find by the inversion of conductivity tensor,  $\hat{R} = \hat{\sigma}^{-1}$ , one also needs to perform the averaging over temperature and over macroscopic spatial inhomogeneities. The macroscopic spatial inhomogeneities result to a spatial variation of the Fermi energy, which is the difference between the chemical potential and the bottom of conducting band. The result for the first harmonic of quantum oscillations does not depend on the order of these two operations: the inversion of conductivity tensor and its averaging. However, the difference (slow) oscillations, even if they are stronger than MQO, appear in the second order of the Dingle factor, and their amplitude and phase depend strongly on the order of these two operations.

The temperature averaging physically corresponds to parallel conductivity channels due to electrons having different energy withing the temperature smearing of Fermi level. Hence, probably, to calculate the resistivity tensor one first needs to perform the temperature averaging of conductivity tensor, and then to invert it. However, for the averaging over macroscopic spatial inhomogeneity the order may be opposite, if the regions of different Fermi energy form a series connection of resistances. In real compounds the regions of various Fermi energy are connected randomly, which is intermediate between the parallel and series connection of resistances, and one can apply various effective medium approximations [60] to describe this regime. For a 2D chess-board or triangular pattern of two types of resistances  $R_{1,2}$  the effective diagonal resistance component is their geometrical average [70],  $R_{eff} = (R_1 R_2)^{1/2}$ , but in a magnetic field this rule may violate because of a large Hall component.

As shown in Sec. IV.1, a similar issue about the averaging of conductivity or resistivity emerges for the monotonic growth of interlayer magnetoresistance in a strong magnetic field [58], which is also a non-linear effect in MQO. Averaging (over MQO period) of interlayer conductivity and resistance gives different results. Note that the averaging of the experimental data on interlayer resistivity gives slightly better agreement between the theory and experiment in quasi-2D organic metal (see Figs. 1 and 2 of [58]), but this observation does not give a general rule of the preferable averaging method.

We suggest that this question about the correct averaging procedure of magnetoresistance can be answered experimentally for any particular physical system, and our formulas in Sec. IV derived for both types of averaging may help to do this. The SO of  $R_{zz}$  described

by Eq. (51) are smaller than those in Eq. (50) by a factor  $\sim 2/\lambda = \hbar \omega_c/(2\pi t_z)$  and have a considerably different phase. This phase of SO can be compared with the phase of the beats of the MQO in Eqs. (73) and (75). The phase difference  $\Delta \phi_{SO}$  of SO given by Eqs. (50) and (51), corresponding to  $\sigma$ -averaging and R-averaging, is rather large:  $\Delta \phi_{SO} \sim \pi/2$ . This can be used to experimentally choose the type of averaging, which describes better a physical system under study. The comparison of the field dependence of the amplitudes and phases of SO of the diagonal  $R_{xx}$  and Hall  $R_{xy}$  resistivity components, described by Eqs. (56)-(58) and (64)-(65), also helps to determine which type of averaging is more suitable for a particular system.

The combined analysis of the magnetic quantum and slow (difference) oscillations of the diagonal and Hall components of intralayer magnetoresistance tensor and of interlayer longitudinal magnetoresistance provides much more useful information about the electronic properties of quasi-2D metals than the measurements of MQO of a single quantity. The analytical formulas for these effects, obtained in Sec. IV, are convenient for the comparison with experimental data. The results obtained also give several qualitative and quantitative predictions on the magnetoresistance oscillations, their relative amplitudes and phases, which can be tested experimentally.

#### VI. SUMMARY

Summing up, in Sec. III we calculated the magnetic quantum and slow oscillations of intralayer Hall conductivity  $\sigma_{xy}$  in quasi-2D metals in a quantizing magnetic field, assuming that the oscillating part is still much smaller than the monotonic part. This calculation is based on the Kubo-Streda formula. The theory takes into account the electron scattering by short-range crystal defects, e.g. by impurities, and neglects the electronelectron interaction. The latter approximation is justified in the metallic limit of a large number of filled LLs and finite interlayer transfer integral  $t_z$ . Previously, similar calculation in quasi-2D metals was performed only for the diagonal components of conductivity [10, 39]. In IV we calculate the intralaver magnetoresistance tensor, which allows a direct comparison with experimental data. The averaging of magnetoresistance over the period of quantum oscillations due to a finite temperature and spatial sample inhomogeneities is nontrivial, as discussed in Sec. IV and V, which is important both for differential slow oscillations and for the monotonic part of magnetoresistance.

The obtained analytical formulas describe the amplitude and phase of the magnetic quantum and slow (difference) oscillations of magnetoresistance tensor as a function of magnetic field strength, temperature, disorder, interlayer transfer integral, and other parameters. They are convenient for the comparison with experiment to extract the electronic parameters of various layered met-

als. They also predict several qualitative and quantitative feature of magnetoresistance oscillations, which can be directly compared with experiment. For example, we predict the non-monotonic field dependence of the amplitude and phase of slow oscillations in a certain range of parameters, the field-dependent phase difference between the oscillations of diagonal and Hall magnetoresistance components, the difference between the MQO of intralayer and interlayer magnetoresistance, etc. The developed theory and its results are useful for describing transport properties in a variety of anisotropic quasi-2D metals, including high-temperature superconductors, rare-earth polytellurides, layered chalcogenides, van-der-Waals crystals, heterostructures, organic metals, etc.

#### VII. ACKNOWLEDGMENTS

The work is supported by the Russian Science Foundation Grant No. 22-42-09018. PDG also acknowledges State assignment No. FFWR-2024-0015 and NUST "MISIS" grant No. K2-2022-025.

### Appendix A: Calculation of $\sigma_{xy}^{II}$

To obtain Eq. (8) we integrate the second term in Eq. (5) by parts

$$\sigma_{\mu\nu}^{II} = \frac{-|e|}{4\pi i} \int_{-\infty}^{+\infty} d\varepsilon \, n_F \left(\varepsilon\right)$$

$$\times Tr \left\langle -2\pi i \frac{d\delta \left(\varepsilon - \hat{H}\right)}{d\varepsilon} \left(\hat{r}_{\mu} \hat{v}_{\nu} - \hat{v}_{\mu} \hat{r}_{\nu}\right) \right\rangle$$

$$= \frac{|e|}{2} \int_{-\infty}^{+\infty} d\varepsilon \, n_F \left(\varepsilon\right) Tr \left\langle \frac{d\delta \left(\varepsilon - \hat{H}\right)}{dB} \frac{\left(\hat{r}_{\mu} \hat{v}_{\nu} - \hat{v}_{\mu} \hat{r}_{\nu}\right)}{-d\hat{H}/dB} \right\rangle.$$
(A1)

For any dispersion with Peierls substitution of the vector potential in the symmetric gauge  $\mathbf{A} = \frac{B_z}{2} (-y, x, 0)$  the derivative of the Hamiltonian

$$\frac{d\hat{H}}{dB_z} = \frac{e}{2c} \left( \hat{v}_x y - \hat{v}_y x \right),\tag{A2}$$

which coincides with  $(-e/2c)(\hat{r}_{\mu}\hat{v}_{\nu}-\hat{v}_{\mu}\hat{r}_{\nu})$  since  $[\hat{r}_x,\,\hat{v}_y]=[\hat{r}_y,\,\hat{v}_x]=0$ . Using  $N(\varepsilon)=\int_{-\infty}^{+\infty}d\varepsilon n_F\left(\varepsilon\right)Tr\left\langle\delta\left(\varepsilon-\hat{H}\right)\right\rangle$  one obtains Eq. (8). This derivation does not depend on electron dispersion and on the number of energy bands.

#### Appendix B: Calculation of $\sigma_{xy}^{I}$

In the self-consistent Born approximation (SCBA) or even in the non-crossing approximation, i.e. neglecting only the diagrams with the intersection of impurity lines, the self-energy part  $\Sigma^R(\varepsilon)$  depends only on electron energy  $\varepsilon$  [56], and the electron Green's function does not depend on  $k_x$ :

$$G_n^R(k_x, k_z, \varepsilon) = G_n^A(k_x, k_z, \varepsilon)^* = \frac{1}{\varepsilon - \epsilon_n(k_z) - \Sigma^R(\varepsilon)},$$
(B1)

where  $\epsilon_n(k_z) = \hbar \omega_c(n+1/2) - 2t_z \cos(k_z d)$  according to Eq. (4). The imaginary part of the Green's function, entering the expression (6) for conductivity, is

$$\operatorname{Im} G_n^R(k_x, k_z, \varepsilon) \equiv \operatorname{Im} G_n^R(k_z, \varepsilon) = -\operatorname{Im} G_n^A(k_z, \varepsilon)$$

$$= (G_n^R(k_z, \varepsilon) - G_n^A(k_z, \varepsilon))/(2i)$$

$$= \frac{\operatorname{Im} \Sigma^R(\varepsilon)}{\left[\varepsilon - \epsilon_n(k_z) - \operatorname{Re} \Sigma^R(\varepsilon)\right]^2 + \left[\operatorname{Im} \Sigma^R(\varepsilon)\right]^2}.$$
 (B2)

The matrix elements  $\langle n', k_x, k_z | \hat{v}_i | k_z, k_x, n \rangle$  of electron velocity  $v_i = p_i/m_*$ , entering to the electric current  $j_i = ev_i = e \partial \epsilon(\mathbf{p}) / \partial p_i$ , in the basis of the Landau-gauge quantum numbers  $\{k_x, k_z, n\}$  of an electron in magnetic field are [71]

$$\langle n', k_x, k_z | \hat{v}_x | k_z, k_x, n \rangle$$

$$= \frac{-\hbar}{\sqrt{2}m_* l_H} \left( \sqrt{n' + 1} \delta_{n, n' + 1} + \sqrt{n'} \delta_{n, n' - 1} \right)$$
(B3)
$$= \frac{-\hbar}{\sqrt{2}m_* l_H} \left( \sqrt{n} \delta_{n, n' + 1} + \sqrt{n + 1} \delta_{n, n' - 1} \right),$$
(B4)

$$\langle n', k_x, k_z | \hat{v}_y | k_z, k_x, n \rangle$$

$$= \frac{i\hbar}{\sqrt{2}m_* l_H} \left( \sqrt{n' + 1} \delta_{n, n' + 1} - \sqrt{n'} \delta_{n, n' - 1} \right)$$
(B5)
$$= \frac{i\hbar}{\sqrt{2}m_* l_H} \left( \sqrt{n} \delta_{n, n' + 1} - \sqrt{n + 1} \delta_{n, n' - 1} \right),$$
(B6)

О

$$\langle n, k_x, k_z | \hat{v}_x | k_z, k_x, n' \rangle$$

$$= \frac{-\hbar}{\sqrt{2}m_* l_H} \left( \sqrt{n+1} \delta_{n'-1, n} + \sqrt{n} \delta_{n'+1, n} \right), \quad (B7)$$

$$\langle n, k_x, k_z | \hat{v}_y | k_z, k_x, n' \rangle$$

$$= \frac{i\hbar}{\sqrt{2}m_* l_H} (\sqrt{n+1} \delta_{n'-1, n} - \sqrt{n} \delta_{n, n'+1}), \qquad (B8)$$

where  $l_H = \sqrt{\hbar c/(eB)} = \sqrt{\hbar/(m_*\omega_c)}$  is the magnetic length. Eqs. (B3) and (B5) can be checked by a direct calculation.

The nonzero matrix elements of electron velocity correspond to the change of LL number only by  $\pm 1$ :

$$\langle n|\hat{v}_{x}|\,n-1\rangle = \frac{-\hbar\sqrt{n}}{\sqrt{2}m_{*}l_{H}};\ \langle n|\hat{v}_{x}|\,n+1\rangle = \frac{-\hbar\sqrt{n+1}}{\sqrt{2}m_{*}l_{H}},$$
 (B9)

and for the  $\hat{v}_y$  component

$$\langle n|\hat{v}_y|\ n-1\rangle = \frac{-i\hbar\sqrt{n}}{\sqrt{2}m_*l_H};\ \langle n|\hat{v}_y|\ n+1\rangle = \frac{i\hbar\sqrt{n+1}}{\sqrt{2}m_*l_H}. \tag{B10}$$

From Eqs. (B9) and (B10) one easily obtains the product of the matrix elements of electron velocity:

$$\langle n|\hat{v}_x| \, n - 1\rangle \, \langle n - 1|\hat{v}_y| \, n\rangle = \frac{-i\hbar^2 n}{2m_*^2 l_H^2},$$
 (B11)

$$\left\langle n|\hat{v}_{x}|\,n+1\right\rangle \left\langle n+1|\hat{v}_{y}|\,n\right\rangle =\frac{i\hbar^{2}\left(n+1\right)}{2m_{*}^{2}l_{H}^{2}}.\tag{B12}$$

Substituting  $\hat{\jmath}_{\mu} = e\hat{v}_{\mu}$  into the Eq. (6) leads to

$$\sigma_{xy}^{I}\left(\varepsilon\right) = \frac{\hbar e^{2}}{4\pi} Tr\left\langle \hat{v}_{x}\left(G^{R} - G^{A}\right) \hat{v}_{y} G^{R} - \hat{v}_{x} G^{A} \hat{v}_{y}\left(G^{R} - G^{A}\right)\right\rangle.$$
(B13)

The first term in the Eq. (B13) gives

$$\begin{split} \left\langle n|\hat{v}_{x}\left(G^{R}-G^{A}\right)\hat{v}_{y}G^{R}|n\right\rangle \\ &=\left\langle n|\hat{v}_{x}|n-1\right\rangle \left\langle n-1|\hat{v}_{y}|n\right\rangle G_{n}^{R}\left(G_{n-1}^{R}-G_{n-1}^{A}\right) \\ &+\left\langle n|\hat{v}_{x}|n+1\right\rangle \left\langle n+1|\hat{v}_{y}|n\right\rangle G_{n}^{R}\left(G_{n+1}^{R}-G_{n+1}^{A}\right) \\ &=\frac{-i\hbar^{2}}{2m_{*}^{2}l_{H}^{2}}n\left(G_{n-1}^{R}-G_{n-1}^{A}\right)G_{n}^{R} \\ &+\frac{i\hbar^{2}}{2m_{*}^{2}l_{H}^{2}}\left(n+1\right)\left(G_{n+1}^{R}-G_{n+1}^{A}\right)G_{n}^{R}. \end{split} \tag{B14}$$

The second term in the Eq. (B13) gives

$$\langle n | \hat{v}_{x} G^{A} \hat{v}_{y} \left( G^{R} - G^{A} \right) | n \rangle$$

$$= \langle n | \hat{v}_{x} | n - 1 \rangle \langle n - 1 | \hat{v}_{y} | n \rangle G_{n-1}^{A} \left( G_{n}^{R} - G_{n}^{A} \right)$$

$$+ \langle n | \hat{v}_{x} | n + 1 \rangle \langle n + 1 | \hat{v}_{y} | n \rangle G_{n+1}^{A} \left( G_{n}^{R} - G_{n}^{A} \right)$$

$$= \frac{-i\hbar^{2}}{2m_{*}^{2}l_{H}^{2}} n \left( G_{n}^{R} - G_{n}^{A} \right) G_{n-1}^{A}$$

$$+ \frac{i\hbar^{2}}{2m_{*}^{2}l_{H}^{2}} (n+1) \left( G_{n}^{R} - G_{n}^{A} \right) G_{n+1}^{A}.$$
(B15)

With the help of Eqs. (B14) and (B15) one can rewrite the Eq. (6) as

$$\begin{split} \sigma_{xy}^{I} &= \frac{\hbar e^{2}}{4\pi} Tr \left\langle \hat{v}_{x} \left( G^{R} - G^{A} \right) \hat{v}_{y} G^{R} - \hat{v}_{x} G^{A} \hat{v}_{y} \left( G^{R} - G^{A} \right) \right\rangle \\ &= \frac{i e^{2} \hbar^{3}}{8\pi m_{*}^{2} l_{H}^{2}} \sum_{n, k_{z}} \left[ -n \left( G_{n-1}^{R} - G_{n-1}^{A} \right) G_{n}^{R} \right. \\ &+ \left. \left( n+1 \right) \left( G_{n+1}^{R} - G_{n+1}^{A} \right) G_{n}^{R} + n \left( G_{n}^{R} - G_{n}^{A} \right) G_{n-1}^{A} \right. \\ &\left. - \left( n+1 \right) \left( G_{n}^{R} - G_{n}^{A} \right) G_{n+1}^{A} \right] \end{split} \tag{B16}$$

In this formula the Green's functions  $G_n^{R,A}$  depend both on the LL number n and on the band index  $k_z$ , because the dispersion  $\epsilon_n(k_z)$  depends on  $k_z$ . We now redefine

the summation index  $n \to n+1$  in the first and third terms in the square brackets of Eq. (B16), which gives

$$\sigma_{xy}^{I} = \frac{ie^{2}\hbar^{3}}{8\pi m_{*}^{2}l_{H}^{2}} \sum_{n, k_{z}} \left[ -(n+1) \left( G_{n}^{R} - G_{n}^{A} \right) G_{n+1}^{R} + (n+1) \left( G_{n+1}^{R} - G_{n+1}^{A} \right) G_{n}^{R} + (n+1) \left( G_{n+1}^{R} - G_{n+1}^{A} \right) G_{n}^{A} - (n+1) \left( G_{n}^{R} - G_{n}^{A} \right) G_{n+1}^{A} \right].$$
(B17)

Substituting Eqs. (B1), (B2) into (B17) we get

$$\sigma_{xy}^{I} = \frac{-e^{2}\hbar^{3}}{2\pi m_{*}^{2}l_{H}^{2}} \sum_{n,k_{z}} (n+1) \times$$

$$\left[ \frac{-\operatorname{Im}\Sigma^{R}(\varepsilon)}{\left[\varepsilon - \epsilon_{n+1}(k_{z}) - \operatorname{Re}\Sigma^{R}(\varepsilon)\right]^{2} + \left[\operatorname{Im}\Sigma^{R}(\varepsilon)\right]^{2}} \right] \times \frac{\varepsilon - \epsilon_{n}(k_{z}) - \operatorname{Re}\Sigma^{R}(\varepsilon)}{\left[\varepsilon - \epsilon_{n}(k_{z}) - \operatorname{Re}\Sigma^{R}(\varepsilon)\right]^{2} + \left[\operatorname{Im}\Sigma^{R}(\varepsilon)\right]^{2}} - \frac{-\operatorname{Im}\Sigma^{R}(\varepsilon)}{\left[\varepsilon - \epsilon_{n}(k_{z}) - \operatorname{Re}\Sigma^{R}(\varepsilon)\right]^{2} + \left[\operatorname{Im}\Sigma^{R}(\varepsilon)\right]^{2}} \times \frac{\varepsilon - \epsilon_{n+1}(k_{z}) - \operatorname{Re}\Sigma^{R}(\varepsilon)}{\left[\varepsilon - \epsilon_{n+1}(k_{z}) - \operatorname{Re}\Sigma^{R}(\varepsilon)\right]^{2} + \left[\operatorname{Im}\Sigma^{R}(\varepsilon)\right]^{2}} \right].$$
(B19)

The first and the second terms in Eq. (B19) have the same denominator, and we simplify it to

$$\begin{split} \sigma_{xy}^{I} &= \frac{e^{2}\hbar^{3}}{2\pi m_{*}^{2}l_{H}^{2}} \sum_{n,\,k_{z}} \frac{(n+1)\operatorname{Im}\Sigma^{R}(\varepsilon)}{\left[\varepsilon - \epsilon_{n+1}(k_{z}) - \operatorname{Re}\Sigma^{R}(\varepsilon)\right]^{2} + \left[\operatorname{Im}\Sigma^{R}(\varepsilon)\right]^{2}} \\ &\times \frac{\epsilon_{n+1}(k_{z}) - \epsilon_{n}(k_{z})}{\left[\varepsilon - \epsilon_{n}(k_{z}) - \operatorname{Re}\Sigma^{R}(\varepsilon)\right]^{2} + \left[\operatorname{Im}\Sigma^{R}(\varepsilon)\right]^{2}}. \end{split} \tag{B20}$$

Using the expression for  $\sigma_{xx}$  in Eq. (24) of Ref. [71],

$$\sigma_{xx} = \frac{e^2 \hbar^3}{\pi m_*^2 l_H^2} \sum_{n, k_z} \frac{(n+1) \operatorname{Im} \Sigma^R(\varepsilon)}{\left[\varepsilon - \epsilon_{n+1}(k_z) - \operatorname{Re} \Sigma^R(\varepsilon)\right]^2 + \left[\operatorname{Im} \Sigma^R(\varepsilon)\right]^2} \times \frac{\operatorname{Im} \Sigma^R(\varepsilon)}{\left[\varepsilon - \epsilon_n(k_z) - \operatorname{Re} \Sigma^R(\varepsilon)\right]^2 + \left[\operatorname{Im} \Sigma^R(\varepsilon)\right]^2}, \quad (B21)$$

and noting that  $(\epsilon_{n+1}(k_z) - \epsilon_n(k_z)) / |\mathrm{Im}\Sigma^R(\varepsilon)| = 2\omega_c \tau$  and  $\mathrm{Im}\Sigma^R(\varepsilon) = -|\mathrm{Im}\Sigma^R(\varepsilon)|$ , we reduce Eq. (B20) to Eq. (9):  $\sigma^I_{xy} = -\omega_c \tau \sigma_{xx}$ .

# Appendix C: Harmonic expansion of the electron density of states and the total electron number

The electron DoS per each spin component is given by the sum over Landau levels:

$$\rho_e(\varepsilon) = -\frac{\operatorname{Im} G^R(\varepsilon)}{\pi} = \sum_{n=0}^{+\infty} \sum_{k_z} \operatorname{Im} \frac{N_{LL}/\pi}{\varepsilon - \epsilon(n, k_z) + i0}$$
$$= \sum_{n=0}^{+\infty} \frac{N_{LL}/(\pi d)}{\sqrt{4t_z^2 - (\varepsilon - \hbar\omega_c(n + 1/2))^2}}, \quad (C1)$$

where  $N_{LL} \equiv B|e|/(2\pi\hbar c)$  is the LL degeneracy per one spin component in 2D, coming from the summation over  $k_y$ . When the expression inside the square root becomes negative, the total expression should always be taken equal to zero, because the DoS  $\rho_e$  is a real quantity. To find the MQO one usually transforms sum over LLs in the DoS given by Eq. (C1) to the sum over harmonics using the Poisson summation formula:

$$\sum_{n=n_0}^{+\infty} f(n) = \sum_{k=-\infty}^{+\infty} \int_a^{+\infty} e^{2\pi i k n} f(n) \, dn \,, \tag{C2}$$

where  $a \in (n_0 - 1, n_0)$ . Taking a = 0, below the lowest n = 0 LL, one obtains

$$\rho_e(\varepsilon) = \frac{\rho_0}{\pi} \sum_{k=-\infty}^{+\infty} \int_0^{+\infty} \frac{dn \, \exp\left(2\pi i k \, (n-1/2)\right)}{\sqrt{\left(\frac{2t_z}{\hbar \omega_c}\right)^2 - \left(\frac{\varepsilon}{\hbar \omega_c} - n\right)^2}}, \quad (C3)$$

where  $\rho_0 = N_{LL}/(\hbar\omega_c d)$  is the average DoS at the Fermi level. To proceed further one assumes the Fermi energy  $\mu \gg t_z$ ,  $\hbar\omega_c$ . Since only the LLs with energy  $|\hbar\omega_c(n+1/2) - \mu| < 2t_z$  and  $n \gg 1$  contribute to the DoS at the Fermi level  $\rho(\mu)$ , the latter is not sensitive to the lower integration limit over n. Then to find  $\rho(\mu)$  analytically, one extends the integration over n in Eq. (C3) from  $(0, +\infty)$  to  $(-\infty, +\infty)$ . As a result one replaces  $\rho_e(\varepsilon)$ , which is nonzero only at  $\varepsilon > \hbar\omega_c/2 - 2t_z$ , by  $\rho(\varepsilon)$  given by the well-known formula [54]

$$\rho(\varepsilon) = \sum_{n=-\infty}^{+\infty} \frac{N_{LL}/(\pi d)}{\sqrt{4t_z^2 - (\varepsilon - \hbar\omega_c (n+1/2))^2}}$$
(C4)  
$$= \frac{\rho_0}{\pi} \sum_{k=-\infty}^{+\infty} \int_{-\infty}^{+\infty} \frac{dn \exp(2\pi i k (n-1/2))}{\sqrt{\left(\frac{2t_z}{\hbar\omega_c}\right)^2 - \left(\frac{\varepsilon}{\hbar\omega_c} - n\right)^2}}$$
$$= \rho_0 \sum_{k=-\infty}^{+\infty} (-1)^k \exp\left(\frac{2\pi i k\varepsilon}{\hbar\omega_c}\right) J_0\left(\frac{4\pi kt}{\hbar\omega_c}\right).$$
(C5)

Keeping only zeroth and first harmonics in this expression one obtains Eq. (14). Contrary to  $\rho_e(\varepsilon)$ ,  $\rho(\varepsilon)$  given by Eqs. (C5) or (14) is nonzero at  $\varepsilon < \hbar \omega_c/2 - 2t_z$ .

The above extension of the lower integration limit and of the DoS  $\rho_e(\varepsilon) \to \rho(\varepsilon)$  to negative energy  $\varepsilon$  below the bottom of the conducting band needs some care when the integrals over DoS  $\rho(\varepsilon)$  are involved, as in Eq. (31) for the total electron density, or in the calculation of the thermodynamic potential and magnetization [54, 72, 73]. Evidently, the result in Eq. (31) depends on the lower integration limit over  $\varepsilon$ , contrary to  $a \in (n_0 - 1, n_0)$  in Eqs. (C2), (C3). The correct starting expression for the total electron density is

$$N = \int_{-\infty}^{+\infty} \rho_e(\varepsilon) n_F(\varepsilon) d\varepsilon \approx \int_{-\infty}^{\mu} \rho_e(\varepsilon) d\varepsilon$$
 (C6)

with  $\rho_e(\varepsilon)$  given by Eq. (C1). The last approximate equality in Eq. (C6) holds at low and temperature T as

compared to LL separation  $\hbar\omega_c$ . It also holds at arbitrary T when the chemical potential is just on the maxima or minima of the DoS  $\rho(\varepsilon)$ . However, the last approximate equality in Eq. (C6) may slightly violate at  $T \sim \hbar\omega_c$  when the chemical potential deviates from the extrema of the DoS  $\rho(\varepsilon)$ , so that the latter contains an odd term as a function of  $\varepsilon - \mu$ .

The replacement of  $\rho_e(\varepsilon)$  in Eq. (C6) by  $\rho(\varepsilon)$  from Eqs. (C5) or (14) gives  $N = +\infty$ . More importantly, the magnetic field derivative in Eq. (32) then oscillates as a function of the lower integration limit in Eqs. (31) or (C6) with the period of MQO without a definite value. This problem can be solved by the observation that

$$N \approx \int_{-\infty}^{\mu} \rho_e(\varepsilon) d\varepsilon = \int_{0}^{\mu} \rho(\varepsilon) d\varepsilon.$$
 (C7)

The difference

$$\delta N = \int_{-\infty}^{\mu} \rho_e(\varepsilon) d\varepsilon - \int_{0}^{\mu} \rho(\varepsilon) d\varepsilon \tag{C8}$$

after the substitution of Eqs. (C1) and (C4) becomes

$$\delta N = \int_{-\infty}^{\mu} \sum_{n=0}^{+\infty} \frac{N_{LL}/(\pi d)}{\sqrt{4t_z^2 - (\varepsilon - \hbar\omega_c (n+1/2))^2}} d\varepsilon \quad (C9)$$
$$-\int_0^{\mu} \sum_{n=-\infty}^{+\infty} \frac{N_{LL}/(\pi d)}{\sqrt{4t_z^2 - (\varepsilon - \hbar\omega_c (n+1/2))^2}} d\varepsilon.$$

Both integrals in Eq. (C9) contain the same terms

$$\int_{0}^{\mu} \sum_{n=0}^{+\infty} \frac{N_{LL}/(\pi d)}{\sqrt{4t_{z}^{2} - (\varepsilon - \hbar\omega_{c} (n+1/2))^{2}}} d\varepsilon,$$

which cancel each other. Then Eq. (C9) rewrites as

$$\delta N = \int_{-\infty}^{0} \sum_{n=0}^{+\infty} \frac{N_{LL}/(\pi d)}{\sqrt{4t_z^2 - (\varepsilon - \hbar\omega_c (n+1/2))^2}} d\varepsilon \quad (C10)$$
$$-\int_{0}^{\mu} \sum_{n=-\infty}^{-1} \frac{N_{LL}/(\pi d)}{\sqrt{4t_z^2 - (\varepsilon - \hbar\omega_c (n+1/2))^2}} d\varepsilon.$$

In quasi-2D metals each LL contributes the electronic DoS in the energy interval  $(-2t_z, 2t_z)$  of  $k_z$ -dispersion bandwidth  $4t_z$ . Therefore, each sum over n in Eq. (C10) contains only  $n_t$  nonzero terms, where  $n_t$  is the smallest integer greater than or equal to  $2t_z/\hbar\omega_c-1/2$ . Moreover, the sum in the second line of Eq. (C10) is nonzero only at  $\varepsilon < 2t_z - \hbar\omega_c/2 \ll \mu$ , and the upper integration limit in the second line of Eq. (C10) can be extended from  $\mu$  to  $+\infty$ . Then the variable change  $\varepsilon \to -\varepsilon$  and  $n \to -n-1$  identically transforms the second integral in Eq. (C10)

to the first one:

$$\begin{split} & \int_{0}^{+\infty} \sum_{n=-\infty}^{-1} \frac{N_{LL}/(\pi d)}{\sqrt{4t_{z}^{2} - \left(\varepsilon - \hbar\omega_{c}\left(n + 1/2\right)\right)^{2}}} d\varepsilon \\ & \to \int_{-\infty}^{0} \sum_{n=0}^{+\infty} \frac{N_{LL}/(\pi d)}{\sqrt{4t_{z}^{2} - \left(-\varepsilon - \hbar\omega_{c}\left(-n - 1/2\right)\right)^{2}}} d\varepsilon \\ & = \int_{-\infty}^{0} \sum_{n=0}^{+\infty} \frac{N_{LL}/(\pi d)}{\sqrt{4t_{z}^{2} - \left(\varepsilon - \hbar\omega_{c}\left(n + 1/2\right)\right)^{2}}} d\varepsilon. \end{split}$$

Hence, two terms in Eq. (C10) exactly cancel each other, giving  $\delta N = 0$  and proving Eq. (C7). This substantiates Eq. (31) and shows that the low integration limit  $\varepsilon = 0$  in Eq. (31) is the only correct.

- H. Zhang, T. Pincelli, C. Jozwiak, T. Kondo, R. Ernstorfer, T. Sato, and S. Zhou, Nature Reviews Methods Primers 2, 54 (2022).
- [2] D. Shoenberg, Magnetic Oscillations in Metals (Cambridge Monographs on Physics) (Cambridge University Press, 2009).
- [3] A. A. Abrikosov, Fundamentals of the theory of metals (North-Holland Sole distributors for the USA and Canada, Elsevier Science Pub. Co, Amsterdam New York, NY, USA, 1988).
- [4] J. M. Ziman, *Principles of the theory of solids* (Cambridge University Press, Cambridge England, 1972).
- [5] M. V. Kartsovnik, Chem. Rev. 104, 5737 (2004).
- [6] J. Singleton, Rep. Prog. Phys. **63**, 1111 (2000).
- [7] J. Wosnitza, Fermi Surfaces of Low-Dimensional Organic Metals and Superconductors (Springer Berlin, Berlin, 2013).
- [8] M. V. Kartsovnik and V. G. Peschansky, Low Temp. Phys. 31, 185 (2005).
- [9] P. D. Grigoriev, M. V. Kartsovnik, W. Biberacher, N. D. Kushch, and P. Wyder, Phys. Rev. B 65, 060403 (2002).
- [10] P. D. Grigoriev, Phys. Rev. B 67, 144401 (2003).
- [11] T. I. Mogilyuk, P. D. Grigoriev, V. D. Kochev, I. S. Volokhov, and I. Y. Polishchuk, 3D-2D crossover and phase shift of beats of quantum oscillations of interlayer magnetoresistance in quasi-2D metals (2024), arXiv:2405.10174 [cond-mat.str-el].
- [12] M. Schiller, W. Schmidt, E. Balthes, D. Schweitzer, H.-J. Koo, M. H. Whangbo, I. Heinen, T. Klausa, P. Kircher, and W. Strunz, Europhysics Letters 51, 82 (2000).
- [13] M. V. Kartsovnik, P. A. Kononovich, V. N. Laukhin, and I. F. Shchegolev, Sov. Phys.: JETP Lett. 48, 541 (1988).
- [14] K. Yamaji, J. Phys. Soc. Jpn. 58, 1520 (1989).
- [15] R. Yagi, Y. Iye, T. Osada, and S. Kagoshima, J. Phys. Soc. Jpn. 59, 3069 (1990).
- [16] A. G. Lebed, The physics of organic superconductors and conductors (Springer, Berlin, 2008).
- [17] Y. Kurihara, J. Phys. Soc. Jpn. **61**, 975 (1992).
- [18] P. Moses and R. H. McKenzie, Phys. Rev. B 60, 7998 (1999).
- [19] P. D. Grigoriev and T. I. Mogilyuk, Phys. Rev. B 90, 115138 (2014).
- [20] N. E. Hussey, M. Abdel-Jawad, A. Carrington, A. P. Mackenzie, and L. Balicas, Nature 425, 814 (2003).
- [21] M. Kuraguchi, E. Ohmichi, T. Osada, and Y. Shiraki, Synthetic Metals 133-134, 113 (2003), proceedings of the Yamada Conference LVI. The Fourth International Sym-

- posium on Crystalline Organic Metals, Superconductors and Ferromagnets (ISCOM 2001).
- [22] P. D. Grigoriev and T. I. Mogilyuk, Phys. Rev. B 95, 195130 (2017).
- [23] P. D. Grigoriev and T. I. Mogilyuk, J. Phys. Conf. Ser. 1038, 012123 (2018).
- [24] R. Ramazashvili, P. D. Grigoriev, T. Helm, F. Koll-mannsberger, M. Kunz, W. Biberacher, E. Kampert, H. Fujiwara, A. Erb, J. Wosnitza, R. Gross, and M. V. Kartsovnik, npj Quantum Materials 6, 11 (2021).
- [25] M. V. Kartsovnik, V. N. Laukhin, V. I. Nizhankovskii, and A. A. Ignat'ev, Sov. Phys.: JETP Lett. 47, 363 (1988).
- [26] E. Ohmichi, H. Ito, T. Ishiguro, G. Saito, and T. Ko-matsu, Phys. Rev. B 57, 7481 (1998).
- [27] B. Z. Narymbetov, N. D. Kushch, L. V. Zorina, S. S. Khasanov, R. P. Shibaeva, T. G. Togonidze, A. E. Kovalev, M. V. Kartsovnik, L. I. Buravov, E. B. Yagubskii, E. Canadell, A. Kobayashi, and H. Kobayashi, Eur. Phys. J. B 5, 179 (1998).
- [28] T. G. Togonidze, M. V. Kartsovnik, J. A. A. J. Perenboom, N. D. Kushch, and H. Kobayashi, Physica B 294-295, 435 (2001).
- [29] A. A. Sinchenko, P. D. Grigoriev, P. Monceau, P. Lejay, and V. N. Zverev, J. Low Temp. Phys. 185, 657 (2016).
- [30] P. D. Grigoriev, A. A. Sinchenko, P. Lejay, A. Hadj-Azzem, J. Balay, O. Leynaud, V. N. Zverev, and P. Monceau, Eur. Phys. J. B 89, 151 (2016).
- [31] P. D. Grigoriev and T. Ziman, JETP Lett. 106, 371 (2017).
- [32] P. D. Grigoriev and T. Ziman, Phys. Rev. B 96, 165110 (2017).
- [33] M. V. Kartsovnik, P. D. Grigoriev, W. Biberacher, N. D. Kushch, and P. Wyder, Phys. Rev. Lett. 89, 126802 (2002).
- [34] T. Mogilyuk, J. Supercond. Novel Magn. 35, 2175 (2022).
- [35] M. E. Raikh and T. V. Shahbazyan, Phys. Rev. B 49, 5531 (1994).
- [36] N. S. Averkiev, L. E. Golub, S. A. Tarasenko, and M. Willander, Journal of Physics: Condensed Matter 13, 2517 (2001).
- [37] V. Leeb and J. Knolle, Phys. Rev. B 108, 054202 (2023).
- [38] T. Champel and V. P. Mineev, Phys. Rev. B 66, 195111 (2002).
- [39] T. I. Mogilyuk and P. D. Grigoriev, Phys. Rev. B 98, 045118 (2018).
- [40] N. Doiron-Leyraud, C. Proust, D. LeBoeuf, J. Levallois,

- J.-B. Bonnemaison, R. Liang, D. A. Bonn, W. N. Hardy, and L. Taillefer, Nature 447, 565 (2007).
- [41] J. G. Analytis, J.-H. Chu, Y. Chen, F. Corredor, R. D. McDonald, Z. X. Shen, and I. R. Fisher, Phys. Rev. B 81, 205407 (2010).
- [42] M. Busch, O. Chiatti, S. Pezzini, S. Wiedmann, J. Sánchez-Barriga, O. Rader, L. Yashina, and S. Fischer, Sci. Rep. 8, 485 (2018).
- [43] T. Terashima, H. T. Hirose, N. Kikugawa, S. Uji, D. Graf, T. Morinari, T. Wang, and G. Mu, npj Quantum Mater. 7, 1 (2022).
- [44] X. Zhu, H. Yang, L. Fang, G. Mu, and H.-H. Wen, Supercond. Sci. Technol. 21, 105001 (2008).
- [45] T. Higashihara, R. Asama, R. Nakamura, M. Watanabe, N. Tomoda, T. J. Hasiweder, Y. Fujisawa, Y. Okada, T. Iwasaki, K. Watanabe, T. Taniguchi, N. Jiang, and Y. Niimi, Phys. Rev. B 109, 134404 (2024).
- [46] A. A. Sinchenko, P. D. Grigoriev, A. V. Frolov, A. P. Orlov, V. N. Zverev, A. Hadj-Azzem, E. Pachoud, and P. Monceau, Comparative study of magnetic quantum oscillations in Hall and transverse magnetoresistance (2024), arXiv:2403.19463 [cond-mat.str-el].
- [47] L. Landau and E. Lifshitz, Quantum Mechanics: Non-Relativistic Theory, Course of theoretical physics (Pergamon Press, New York, 1991).
- [48] G. D. Mahan, Many-Particle Physics | SpringerLink (Springer, Boston, MA, 2000).
- [49] M. Schiller, W. Schmidt, E. Balthes, D. Schweitzer, H.-J. Koo, M. H. Whangbo, I. Heinen, T. Klausa, P. Kircher, and W. Strunz, Europhys. Lett. 51, 82 (2000).
- [50] H. Weiss, M. V. Kartsovnik, W. Biberacher, E. Balthes, A. G. M. Jansen, and N. D. Kushch, Phys. Rev. B 60, R16259 (1999).
- [51] L. Smrcka and P. Streda, J. Phys. C: Solid State Phys. 10, 2153 (1977).
- [52] K. Chadova, Ludwig-Maximilians-Universität München 10.5282/edoc.21609 (2017).
- [53] P. Streda, J. Phys. C: Solid State Phys. 15, L717 (1982).
- [54] T. Champel and V. P. Mineev, Philos. Mag. B 81, 55 (2001).

- [55] A. Isihara and L. Smrcka, J. Phys. C: Solid State Phys. 19, 6777 (1986).
- [56] P. D. Grigoriev, Phys. Rev. B 83, 245129 (2011).
- [57] P. D. Grigoriev, JETP Lett. **94**, 47 (2011).
- [58] P. D. Grigoriev, M. V. Kartsovnik, and W. Biberacher, Phys. Rev. B 86, 165125 (2012).
- [59] P. D. Grigoriev, Phys. Rev. B 88, 054415 (2013).
- [60] S. Torquato, Random Heterogeneous Materials (Springer New York, 2002).
- [61] S. E. Sebastian and C. Proust, Annual Review of Condensed Matter Physics 6, 411 (2015).
- [62] T. Helm, M. V. Kartsovnik, M. Bartkowiak, N. Bittner, M. Lambacher, A. Erb, J. Wosnitza, and R. Gross, Phys. Rev. Lett. 103, 157002 (2009).
- [63] L. J. Van der Pauw, Philips Research Reports 13, 1 (1958).
- [64] J. Webster, The Measurement, Instrumentation and Sensors Handbook, Electrical Engineering Handbook (Taylor & Francis, 1998).
- [65] H. C. Montgomery, Journal of Applied Physics 42, 2971 (1971), https://pubs.aip.org/aip/jap/articlepdf/42/7/2971/7947133/2971\_1\_online.pdf.
- [66] A. I. Coldea, D. Braithwaite, and A. Carrington, Comptes Rendus Physique 14, 94 (2013).
- [67] A. A. Sinchenko, P. D. Grigoriev, P. Lejay, and P. Monceau, Phys. Rev. B 96, 245129 (2017).
- [68] P. D. Grigoriev, A. A. Sinchenko, P. A. Vorobyev, A. Hadj-Azzem, P. Lejay, A. Bosak, and P. Monceau, Phys. Rev. B 100, 081109 (2019).
- [69] R. Vansweevelt, V. Mortet, J. D'Haen, B. Ruttens, C. Van Haesendonck, B. Partoens, F. M. Peeters, and P. Wagner, Physica status solidi (a) 208, 1252 (2011).
- [70] V. G. Marikhin, Journal of Experimental and Theoretical Physics Letters 71, 271 (2000).
- [71] P. Středa and L. Smrčka, Phys. Status solidi B 70, 537 (1975).
- [72] P. D. Grigoriev, J. Exp. Theor. Phys. 92, 1090 (2001).
- [73] T. Mogilyuk, Journal of Superconductivity and Novel Magnetism 35, 2175 (2022).